



# AirCargoChallenge 2022

# Technical Report

Team #05

Chicken Wings BUT





## CONTENT

1.	INTRODUCTION .....	4
1.1	Main objective .....	4
1.2	Design approach .....	4
2.	PROJECT MANEGEMENT.....	4
2.1	Financial budget.....	4
2.2	Time schedule .....	5
3.	AICRAFT DESIGN .....	6
3.1	Wing concept design.....	7
3.2	Empennage concept design .....	8
3.3	Fuselage concept design .....	9
3.4	Landing gear design .....	9
3.5	Engine and electronic system summary.....	10
3.6	Final design summary .....	11
4.	AERODYNAMIC DESIGN .....	12
4.1	Wing design .....	12
4.2	Tail design .....	15
4.3	Fuselage design.....	16
4.4	Final aerodynamic design.....	16
5.	CENTRE OF GRAVITY DETERMINATION.....	17
6.	PAYLOAD PREDICTION .....	18
7.	FLIGHT PERFORMANCE.....	19
7.1	Thrust measurement .....	19
7.2	Horizontal flight .....	19
7.3	Climb.....	20
7.4	Take off.....	21
8.	STABILITY.....	22
9.	STRUCTURAL DESIGN.....	23
9.1	Flight envelope.....	23
9.2	Wing design .....	24
9.3	Tail design .....	26
9.4	Fuselage and landing gear design .....	28
10.	FINAL DESIGN SUMMARY .....	29
11.	DIFFICULTIES DURING THE PROJECT, INNOVATIONS.....	30
12.	OUTLOOK.....	30



## LIST OF SYMBOLS AND ABBREVIATIONS

<b>UAV</b>	Powered unmanned aerial vehicle	<b>Ty</b>	Shear force
<b>BUT</b>	Brno University of Technology	<b>Mo</b>	Bending moment
<b>FME</b>	Faculty of Mechanical Engineering	<b>Mk</b>	Torsion moment
<b>S</b>	Wing area	<b>M<sub>tow</sub></b>	Maximum take-off weight
<b>l</b>	Wingspan	<b>F</b>	Thrust
<b>c<sub>k</sub></b>	Root profile length	<b>G</b>	Gravity
<b>C<sub>MAC</sub></b>	Mean aerodynamic chord length	<b>L</b>	Lift
<b>x<sub>MAC</sub></b>	MAC position along the wingspan	<b>D</b>	Drag
<b>c<sub>SGT</sub></b>	Mean geometric chord	<b>n</b>	Load factor
<b>S<sub>HT</sub></b>	Horizontal tail area	<b><math>\bar{x}_{AKT}</math></b>	Position of the aerodynamic center of wing- fuselage
<b>S<sub>VT</sub></b>	Vertical tail area	<b><math>\Delta\bar{x}_{HT}</math></b>	Position of the aerodynamic center of horizontal tail
<b>S<sub>T</sub></b>	Total tail area	<b><math>\sigma_A</math></b>	Static reserve
<b>l<sub>tail</sub></b>	Tail span	<b><math>\bar{x}_T</math></b>	CG position due to the C <sub>MAC</sub>
<b>c<sub>tr</sub></b>	Tail root profile length	<b>c<sub>mK</sub></b>	Wing moment coefficient
<b>V<sub>HT</sub></b>	Horizontal tail volume	<b>c<sub>m0K</sub></b>	Wing moment coefficient at zero lift
<b>V<sub>VT</sub></b>	Vertical tail volume	<b><math>\alpha</math></b>	Angle of attack
<b><math>\alpha</math></b>	Angle	<b><math>\alpha_{KT}</math></b>	Angle of attack wing- fuselage
<b>C<sub>Lmax</sub></b>	Maximal lift coefficient	<b><math>\alpha_{0KT}</math></b>	Angle of attack wing- fuselage at zero lift
<b>C<sub>Dmin</sub></b>	Minimal drag coefficient	<b><math>\varphi_K</math></b>	Angle of incidence of wing
<b><math>\Delta c_l</math></b>	Lift increase	<b>c<sub>Dm</sub></b>	Drag coefficient defined for minimum lift coefficient
<b><math>\delta_a</math></b>	Deflection	<b>c<sub>Lm</sub></b>	Lift coefficient defined for minimum drag coefficient
<b><math>\frac{c_{l8}}{(c_{l8})_{th}}</math></b>	Correction factor	<b><math>\bar{x}_A</math></b>	Position of the aerodynamic center of the aircraft
<b>(c<sub>l8</sub>)<sub>th</sub></b>	Lift efficiency of aileron	<b>h<sub>s cr</sub></b>	Construction height of the root
<b>k'</b>	Correction factor	<b>h<sub>ef cr</sub></b>	Effective height of the root
<b>c<sub>l<math>\alpha</math></sub></b>	Lift curve slope	<b>t<sub>web</sub></b>	Web width
<b><math>\alpha_\delta</math></b>	Effective lift parameter	<b>k</b>	Safety factor
<b>x<sub>T</sub></b>	Centre of gravity	<b>s</b>	Distance
<b><math>\eta_1</math></b>	$\eta_1$ - shape and size factor	<b>CG</b>	Centre of Gravity
<b><math>\eta_2</math></b>	$\eta_2$ - correction factor	<b>t</b>	Time
<b><math>\left(\frac{\partial\alpha}{\partial\delta}\right)_0</math></b>	Base efficiency		



## 1. INTRODUCTION

The Chicken Wings team consists of a group of students excited about flying, studying bachelor and master studies in Aircraft Design at the Brno University of Technology (BUT) in Czech Republic. Team members are split into 3 sections: aerodynamics section, strength computations, and construction & manufacturing. The team has attended previous international competitions.

### 1.1 Main objective

This report describes the design process of UAV, designed by the team Chicken Wings for Air Cargo Challenge 2022.

The competition aim is to design an electrically powered unmanned aerial vehicle (also known as UAV) with capability to transport a maximum payload amount while flying as fast as possible for 120 seconds flight time. These two criteria (payload mass and flight distance) have the strongest influence on final score. The UAV also must take off within 60m long grass runway and then climb 100 meters in 60 second (100 meters in 60 second has the best score according to the rules). No external power is allowed for aircraft to take-off. The landing shall take place on the landing field mainly consisted of short cut grass.

### 1.2 Design approach

The design aircraft approach is based on experiences gained in the Air Cargo Challenge 2019 and all the past projects. UAV has been fully designed within student's semester projects and bachelor's theses at Faculty of Mechanical Engineering at Brno University of Technology.

For the aircraft key requirements are selected:

- Minimal construction weight,
- Transport maximum weight (payload),
- Climb performance
- Good accessibility of cargo bay,
- Minimal aerodynamic resistance,
- Good construction strength and attention to detail.

## 2. PROJECT MANAGEMENT

This chapter gives a short insight into the project management problematic. Two main project management tasks will be discussed. Namely the question of financial budget and time schedule of the project.

### 2.1 Financial budget

From the beginning of the project, the fixed financial budget has not been set. The team must answer to the question of financing of the project by searching for the suitable sponsors, mainly from the aerospace and aircraft model industry. There was some pre-arranged cooperation from the last years which made the whole process easier. In the meantime, financing of the application fees was covered by the Faculty of Mechanical Engineering at the Brno University of Technology (FME at BUT). There are a several companies that expressed an interest in participating at the project through financial or material sponsorship gifts.

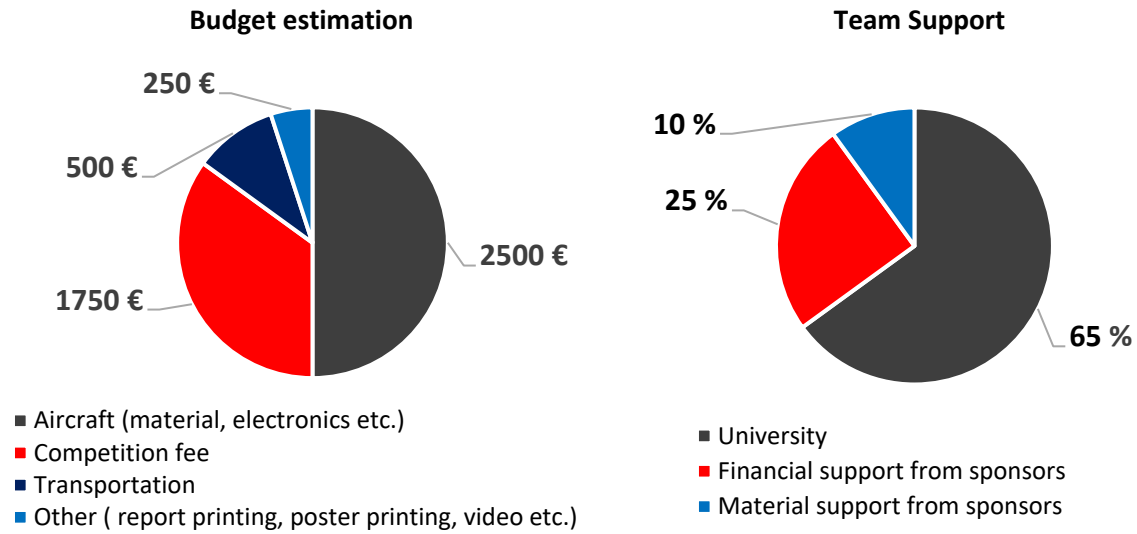


Fig. 2-1 Budget

## 2.2 Time schedule

The basic aircraft development processes time schedule is included in the Gant diagram below. However, other non-technical activities (e.g., negotiations with sponsors, marketing activities, report writing) run in parallel to the aircraft design and manufacture.

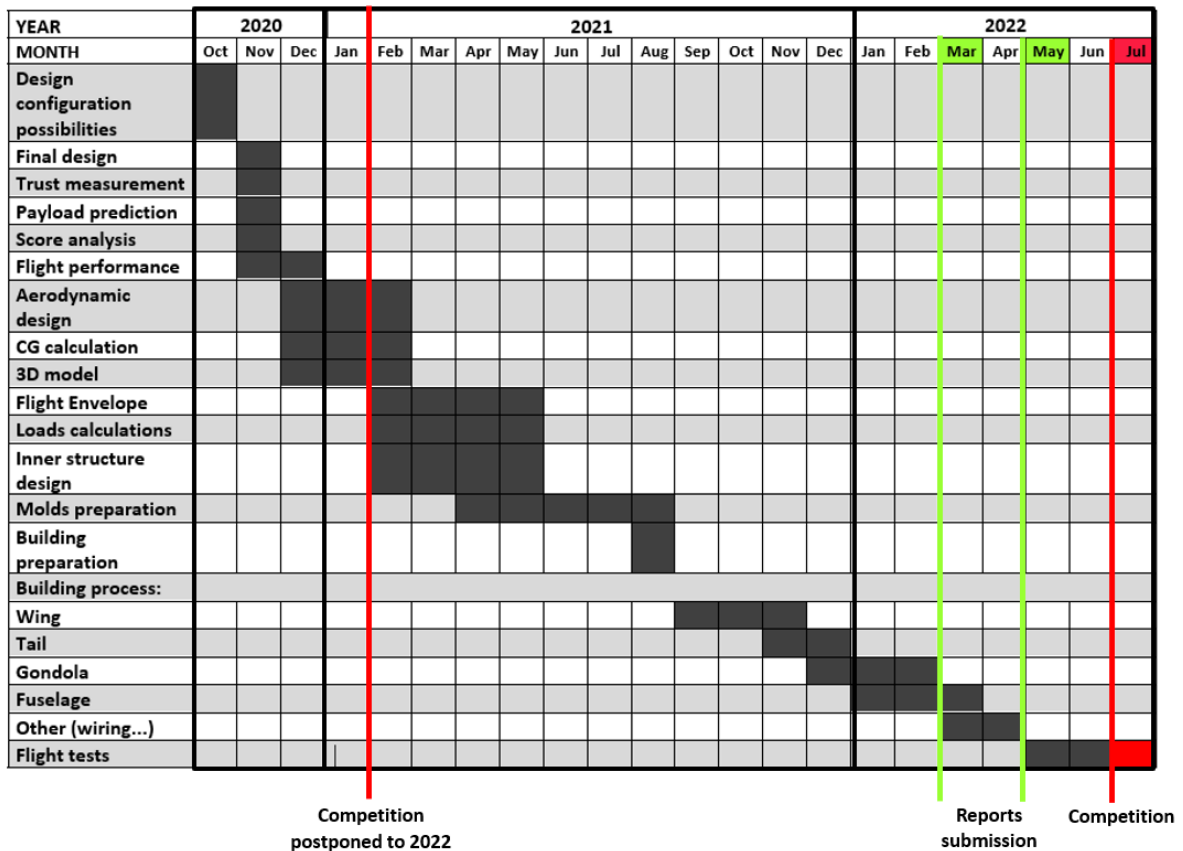


Fig. 2-2 Timetable



### 3. AIRCRAFT DESIGN

Selecting the most sufficient aircraft configuration is critical step which cause success or failure of whole project. Configuration was selected to fulfil the basic assumptions mentioned in chapter 1.2.

The required wing area, the entire aircraft weight, the required lift coefficient were determined by a comprehensive analysis and flight performance calculation. Basic flight performance characteristics are shown in Chapter 7.

Proposed parameters:

- Wing area = 0.5 m<sup>2</sup>
- Preliminary airplane weight m = 5 kg

Fig. 3-1 displays overview of considered aircraft configurations. Final configuration is described in following subchapters.

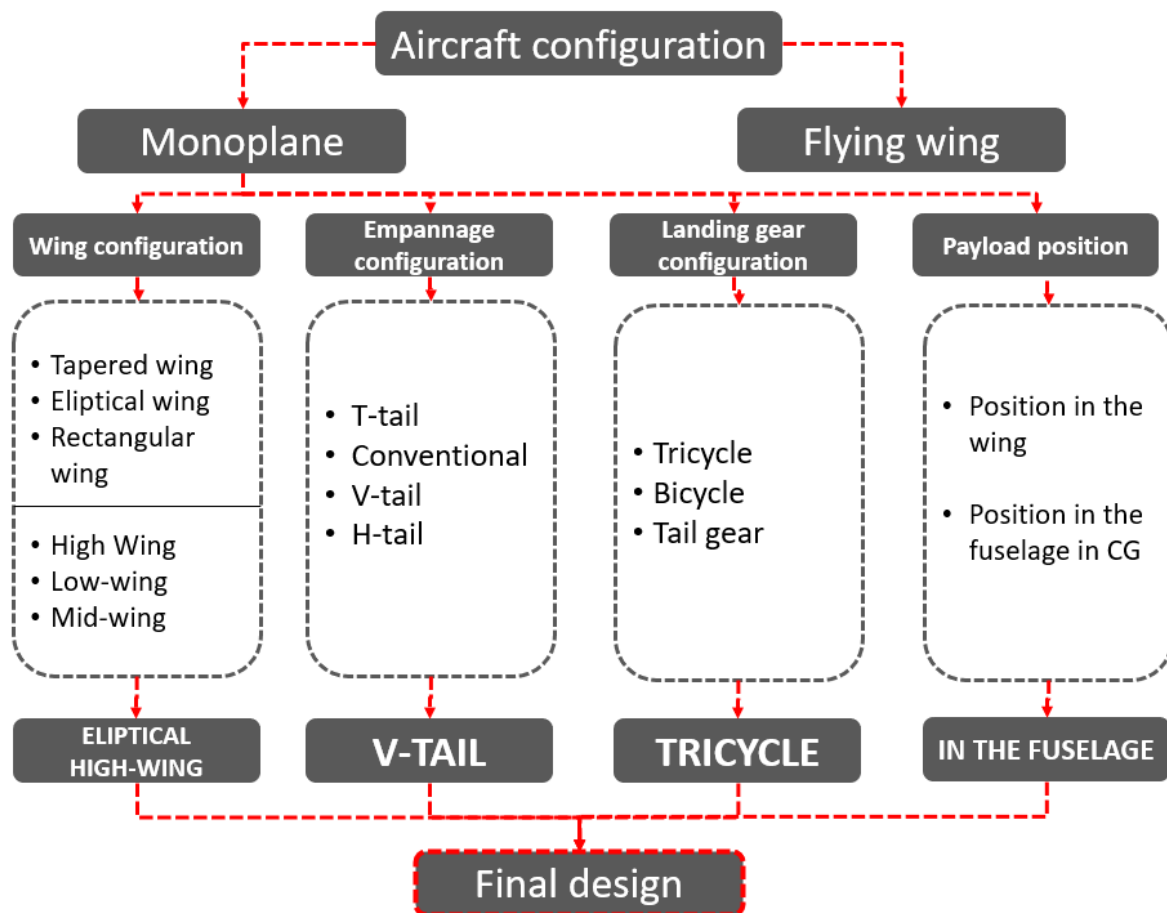


Fig. 3-1 Aircraft configuration

It is the airplane placement in the ready to flight box that influences the entire conceptual model design. The final placement is displayed in Fig.3-1. Selected wing position allows enough wingspan and provides enough space in backward for tail unit and in the front for engine.

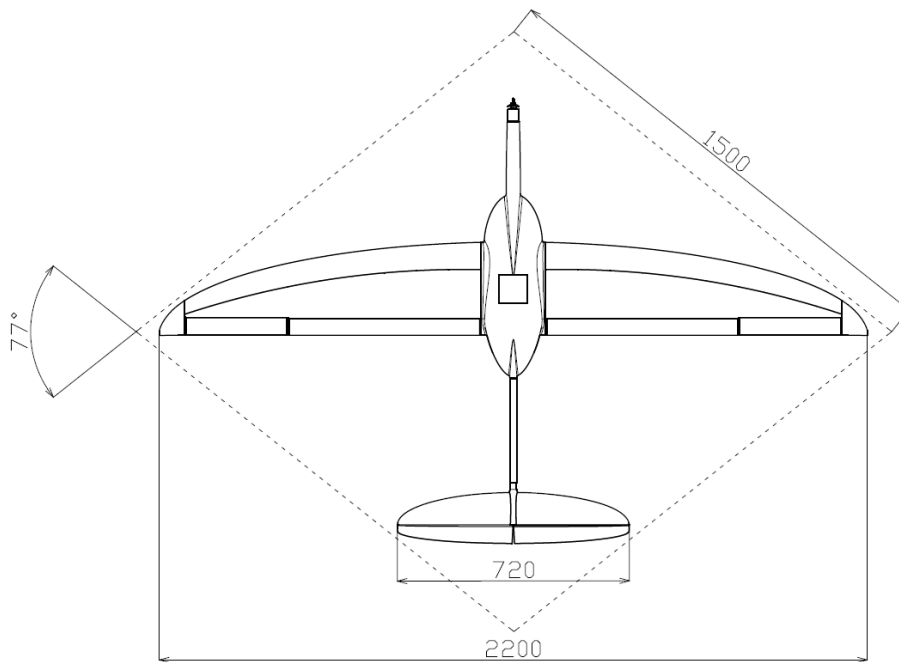


Fig. 3-2 Aircraft position in ready to flight box

### 3.1 Wing concept design

Elliptical wing: It is the most efficient design. The lowest possible induced drag is provided by elliptical wing type, which enables reaching the best possible aspect ratio.

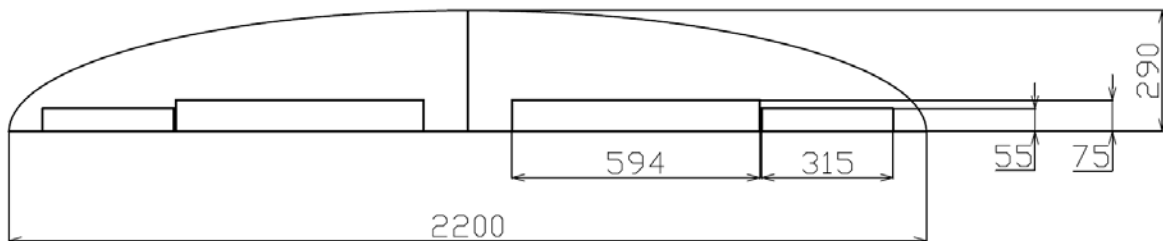


Fig. 3-3 Wing geometry

Mean geometric chord  $c_{SGT}$

$$c_{SGT} = \frac{S}{l} \quad [mm] \quad (3.1)$$

Mean aerodynamic chord (MAC)

Length

$$c_{MAC} = \frac{2}{S} \int_0^{l/2} c^2(y) dy \quad [mm] \quad (3.2)$$

MAC position along the wingspan:

$$x_{MAC} = \frac{2}{S} \int_0^{l/2} c(y)x(y) dy \quad [mm] \quad (3.3)$$

Aspect ratio:

$$\lambda = \frac{l^2}{S} \quad [-] \quad (3.4)$$



Tab. 3.1 Wing geometric parameters

Parameter		Value	
Wing area	$S$	0,5	m <sup>2</sup>
Wingspan	$l$	2200	mm
Root air foil length	$c_k$	290	mm
Mean aerodynamic chord length	$C_{MAC}$	246	mm
MAC position along the wingspan	$x_{MAC}$	467,4	mm
Mean geometric chord	$C_{SGT}$	227,27	mm
Aspect ratio	$\lambda$	9,66	-

### 3.2 Empennage concept design

V –tail: V -tail design is lighter than the other empennage designs. The V-tail is constructed for a lower induced drag. Better stability is caused by two divided areas of the tail. The horizontal and vertical tail area was determined by dimensional limitations and experience from previous years of the ACC competition.

Tab. 3.2 Empennage geometric parameters

Parameter		Value	
Horizontal tail area	$S_{HT}$	0,077	m <sup>2</sup>
Vertical tail area	$S_{VT}$	0,033	m <sup>2</sup>
Total tail area	$S_T$	0,11	m <sup>2</sup>
Tail span	$l_{tail}$	720	mm
Tail root chord length	$c_{tr}$	158	mm

Vertical stabilizer arm is identical to the horizontal stabilizer arm

$$l_{HT0,25} = l_{VT0,25}$$

Subsequently, the remaining quantities were calculated.

Horizontal tail volume:

$$V_{HT} = \frac{S_{HT} \cdot l_{HT0,25}}{S \cdot c_{MAC}} \quad (3.5)$$

Vertical tail volume:

$$V_{VT} = \frac{S_{VT} \cdot l_{VT0,25}}{S \cdot c_{MAC}} \quad (3.6)$$

The deviation tail angle from lateral aircraft axis:

$$\alpha = \arctg \sqrt{\frac{S_{VT}}{S_{HT}}} \quad (3.7)$$

Tab. 3.3 Empennage volumes

Parameter		Value	
Horizontal tail volume	$V_{HT}$	0,4651	-
Vertical tail volume	$V_{VT}$	0,0223	-
Angle	$\alpha$	33	°

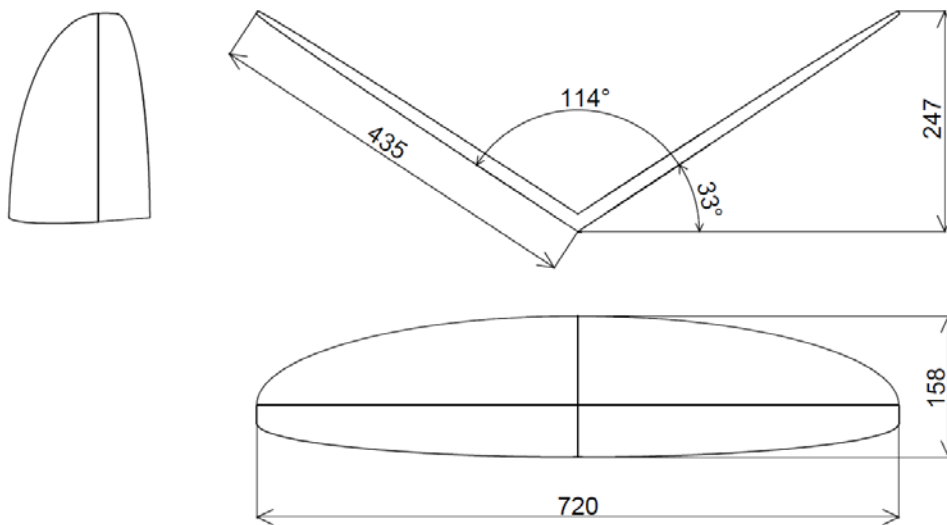


Fig. 3-4 Empennage geometry

### 3.3 Fuselage concept design

The fuselage was divided into two parts to secure position in transportation box. In the front and middle part, which are connected, all the necessary electronics and paying loads are stored. The rear part serves to connect the tail surfaces with the front of the fuselage. Fuselage middle part design is created with respect to the cargobay dimensions. The payload prediction and cargobay design is closely described in Chapter 6.

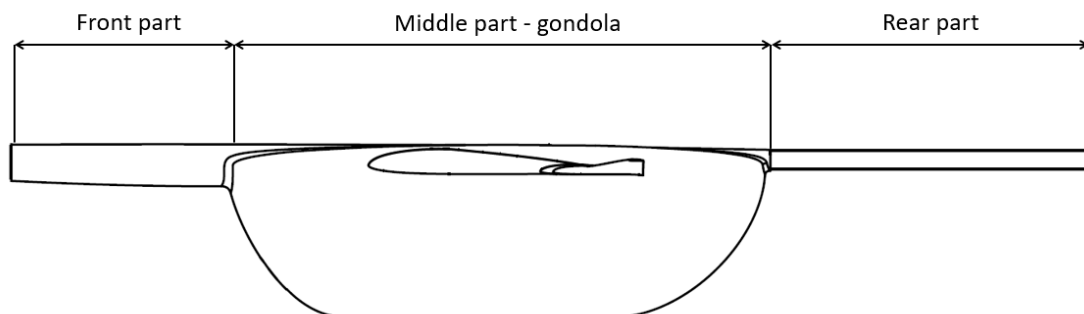


Fig. 3-5 Fuselage concept

### 3.4 Landing gear design

Tricycle landing gear is chosen as landing gear. Dimensions and preview are displayed on the Fig. 3-6.

The airplane landing gear should meet the following specifications to meet safety:

- Simplicity of construction to reduce the risk of failure
- Low weight while ensuring sufficient strength and rigidity, usually should range from 4-8% of the aircraft weight
- Ensuring a sufficient distance of all parts of the aircraft from the ground
- Sufficient static and dynamic stability
- Good manoeuvrability during taxiing and take-off



- Low aerodynamic drag during flight
- Easy maintenance

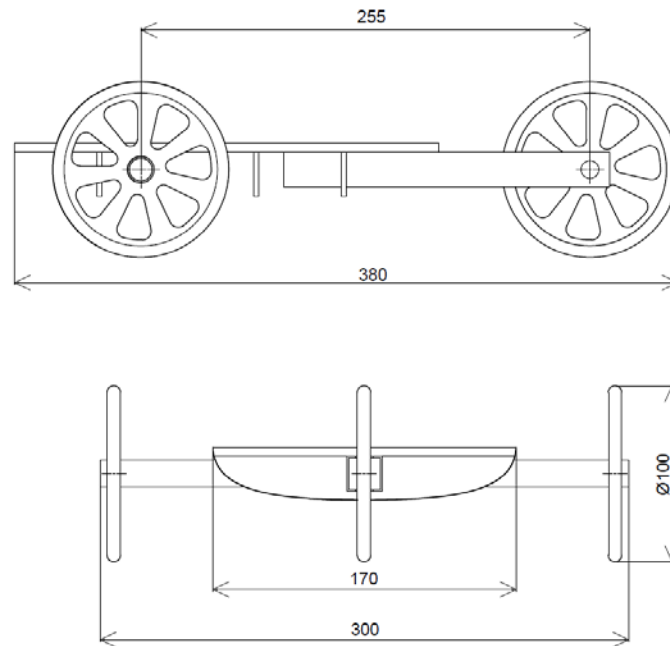
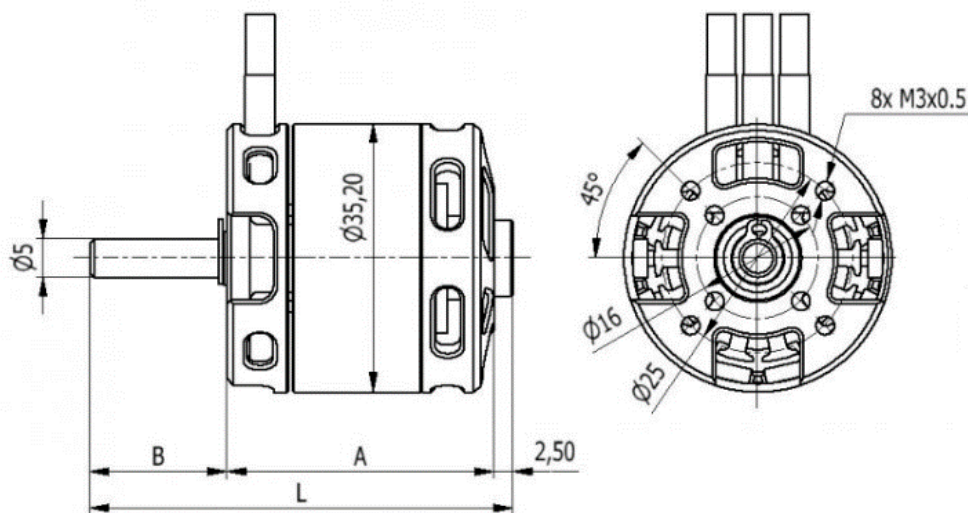


Fig. 3-6 Landing gear geometry

### 3.5 Engine and electronic system summary

According to the rules the motor an unmodified “AXI 2826/10 GOLD LINE V2 must be used. The aircraft is driven by a single motor. The motor is fixed to the airframe of the aircraft.



	A (mm)	B (mm)	L (mm)
AXI-2826	49,4	20	71,9

Fig. 3-7 Engine geometrical parameters [10]

Electronics used in the aircraft meet the criteria described in the competition rules [1]. Electronic scheme is displayed on the Fig. 3-8.



- Motor AXI 2826/10 Gold Line V2 unmodified
- ESC with minimum 30A constant current rating
- LiPo based batteries up to 3 cells
- XT60/XT90 connectors
- KST servo motors

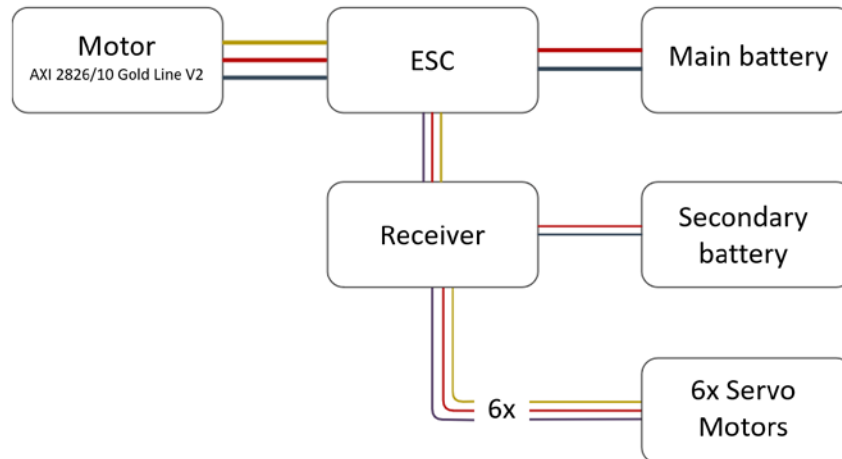


Fig. 3-8 Electronic scheme

### 3.6 Final design summary

High-wing monoplane design was selected because of the possibility to use the fuselage effectively for the payload. Elliptical wing provides the best aerodynamic characteristics. V-tail is chosen because of lowest weight from the possible configurations and configuration allows to fit in the Ready to flight box. The gondola is located under the central wing due to better stability of the plane and better loading access.

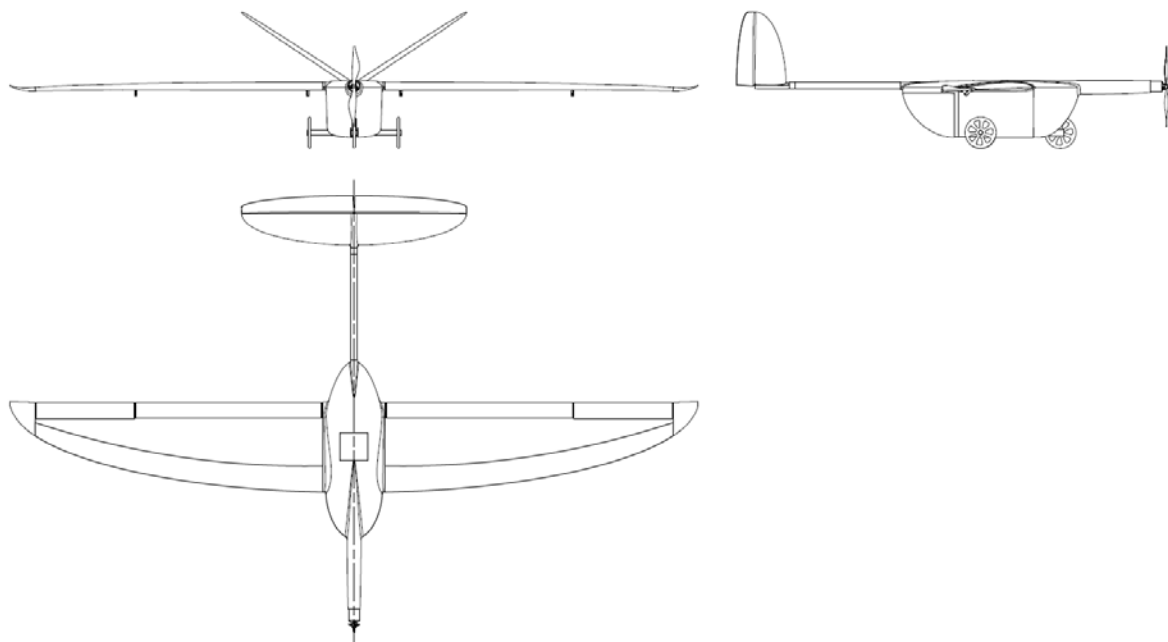


Fig. 3-9 Final design



## 4. AERODYNAMIC DESIGN

### 4.1 Wing design

The airfoil choice—the most important thing in the wing performance is the efficiency and gliding properties, as both have large impact on the overall competition evaluation. It is therefore vital to find a wing airfoil with gliding ratio as high as possible.

The XFLR 5 program was selected for the wing profiles analysis. All selected airfoils were analyzed using XFLR 5. Program is used in the analysis of both aerodynamic wings and entire aircraft at low values of Reynolds numbers. The program uses Lifting line theory (LLT), Vortex Lattice Method and 3D panel method.

Because of the bad stalling properties of the elliptical wing (checked by program Glauert III, developed on BUT, made for the wing stalling characteristics evaluation), the aerodynamic twisting on wing span is implemented.

A combination of s9000 airfoil as the root airfoil and s7075 as the twisted airfoil was selected. The combination reaches the required value  $CL_{max}$  and has a low value  $CD_{min}$ . The  $cL_{\alpha}$  value for the selected wing is 4,095 1/rad. Selected airfoils are shown in Fig.4-1.

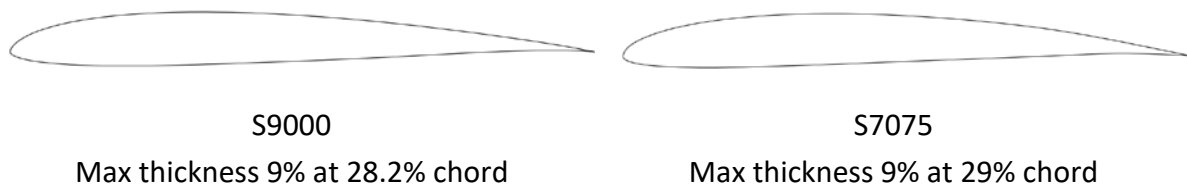


Fig. 4-1 Selected airfoils combination

Tab. 4.1 displays the parameters of the chosen wing, which can be read from the graphs in program XFLR 5. The graphs are displayed on the Fig.4-2. And Fig.4-3.

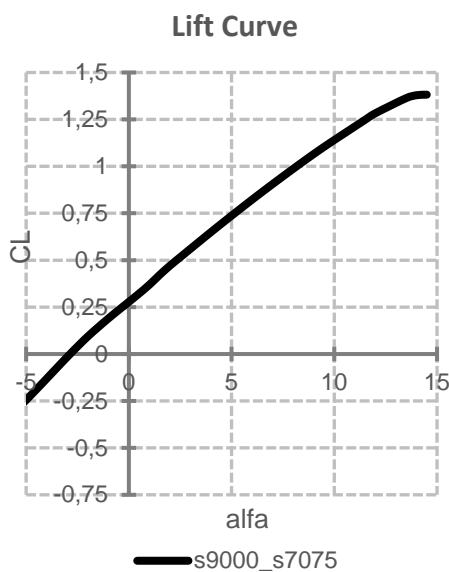


Fig. 4-2 Lift curve

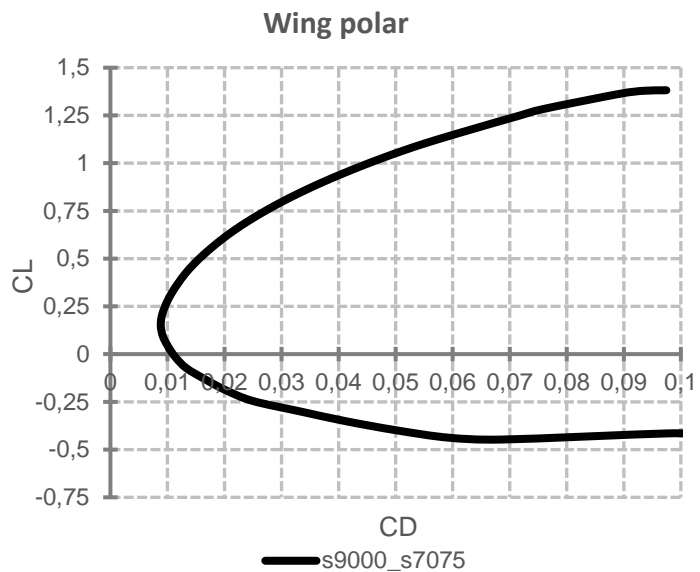


Fig. 4-3 Wing polar



Tab. 4.1 Wing parameters

Characteristics	Profile combination S9000_S7075	
$C_{Lmax}$	1,38	-
Zero angle of attack	-2,86	°
$C_{Dmin}$	0,008	-
Gliding ratio	32,25	-

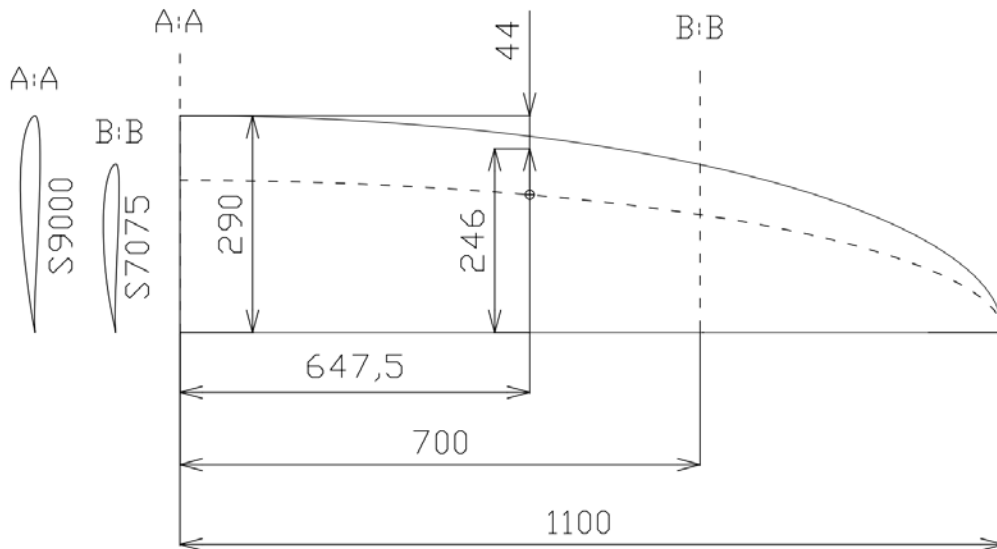


Fig. 4-4 Wing parameters

Lift distribution along the semispan

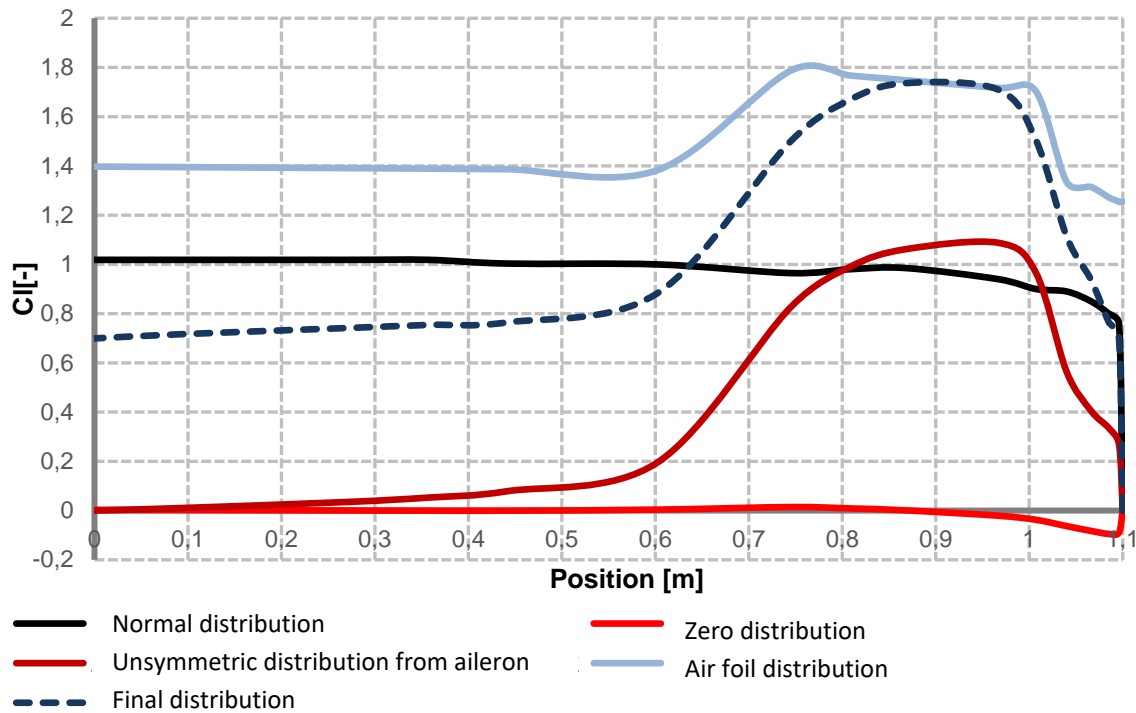


Fig. 4-5 Lift distribution along semispan



- **Wing control surfaces**

High-lift system is very beneficial not only for General aviation aircrafts but for UAV's as well. By adding the mechanism to the wing is possible to influence the lift coefficient ,take-off distance and performance characteristics .

Slotted flaps and plain ailerons combination was chosen.



Fig. 4-6 Control surfaces

Maximum increase in lift coefficient and control surfaces efficiency is calculated according to literature [7]. Only final equations and results are displayed.

The following equation applies to the increase in lift on the airfoil due to the aileron:

$$\Delta c_l = \delta_a \cdot \frac{c_{l\delta}}{(c_{l\delta})_{th}} \cdot (c_{l\delta})_{th} \cdot k' \quad [-] \quad (4.1)$$

where

$\delta_a$	deflection
$\frac{c_{l\delta}}{(c_{l\delta})_{th}}$	correction factor
$(c_{l\delta})_{th}$	lift efficiency of aileron
$k'$	correction factor for nonlinear properties

The increase in lift on the slotted flap is given by the formula:

$$\Delta c_l = c_{l\alpha} \cdot \alpha_\delta \cdot \delta_f \quad (4.2)$$

where

$c_{l\alpha}$	lift curve slope
$\alpha_\delta$	Effective lift parameter

The following equation applies to the efficiency calculation for flap and aileron:

$$\frac{d\alpha}{d\delta} = \eta_1 \cdot \eta_2 \cdot \left( \frac{\partial \alpha}{\partial \delta} \right)_0 \quad [-] \quad (4.3)$$

where

$\eta_1$	shape and size factor
$\eta_2$	correction factor
$\left( \frac{\partial \alpha}{\partial \delta} \right)_0$	base efficiency



Tab. 4.2 Wing control surfaces parameters

Parameter	Flap		Aileron	
Depth	75	mm	55	mm
Length	594	mm	315	mm
Maximum deflection	30	°	±30	°
Flap surface	0,0445	mm <sup>2</sup>	0,0173	mm <sup>2</sup>
Maximum increase in lift coefficient	1,26	-	0,696	-
Efficiency (full deflection)	0,496	-	0,501	-

To increase the lift values during take-off, it is possible to use an aileron. This solution is called a flaperon. For take-off mode, the aileron is set down to a positive deflection. In this way, the coverage of the profile is increased and at the same time the generated lift is increased. However, the aileron deviation is not set to the maximum value due to the controllability of the aircraft.

#### 4.2 Tail design

The symmetrical profile NACA 0010 was chosen for the tail surfaces. The symmetrical airfoil is characterized by the same aerodynamic properties for the positive and negative angle of attack. Main parameter for airfoil selection is low value  $C_{Dmin}$ . According to Fig.4-7 the symmetrical airfoil comparison is made. The NACA 0010 is consider the best solution for the aircraft.

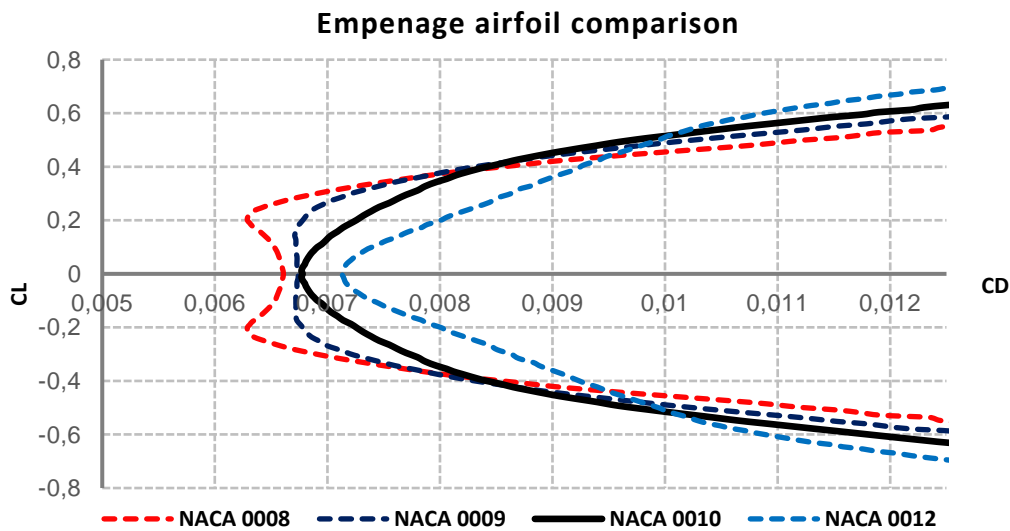


Fig. 4-7 Air foil comparison



Fig. 4-8 NACA 0010



### 4.3 Fuselage design

Based on the knowledge of the cargobay dimensions (payload prediction described in chapter 6.), it was possible to create the geometry of the nacelle and the entire middle part of the fuselage. The effort was to keep the external dimensions as small as possible, given the already sizeable cargo.

The Eppler 863 air foil was chosen and was modified for the needs of the model.

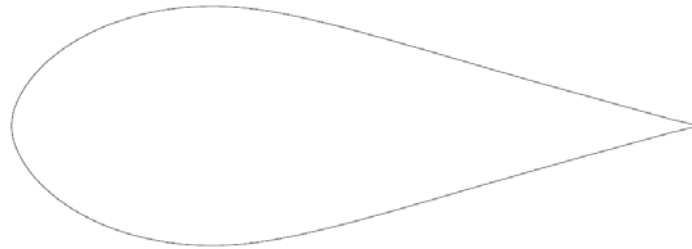


Fig. 4-9 Eppler 863

Final aerodynamic shape of the fuselage middle part is shown on the Fig.4-10.



Fig. 4-10 Fuselage aerodynamic shape

### 4.4 Final aerodynamic design

Final aerodynamic design is calculated in XFLR5. Fig. 4-11 displays the XFLR5 model.

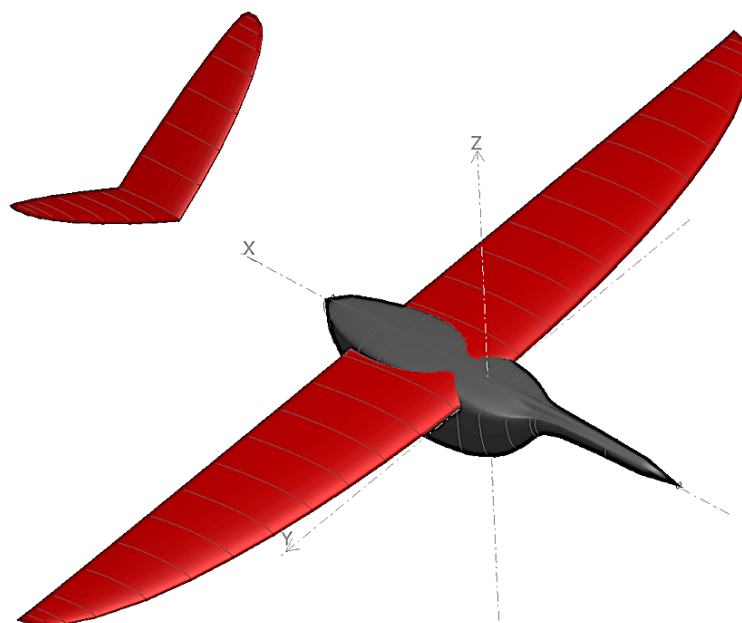


Fig. 4-11 Aircraft in XFLR5



## 5. CENTRE OF GRAVITY DETERMINATION

The centre of gravity determination is one of the most important points in the design process. At the initial design stage, the precise centre of gravity estimation is very difficult because masses of particular aircraft parts and components must be estimated.

Tab. 5.1 CG determination - weights

Item	No.	m [g]	*X [mm]
Payload	1	2100	699,5
Telemetry	2	150	730
Front Fuselage + cargo bay	3	765	684,83
Propeller	4	25	155
Landing gear	5	200	669,99
Engine	6	177	185
Main battery + wiring	7	234	615
Regulator + wiring	8	56	400
Receiver+ wiring	9	22	590
Battery for receiver	10	86	590
Wing	11	840	670
Servo motors in the wing + wiring	12	60	751
Rear fuselage	13	70	1060
Tail unit	14	175	1445
Servo motors in the tail unit + wiring	15	40	1460
<b>Total weight</b>	-	<b>5000</b>	-

\*The coordinate system is located at a distance of 155 mm from propeller. The distance between the origin of the mean aerodynamic chord and the origin of the coordinate system is 625 mm.

$$x_{aer} = 625mm$$

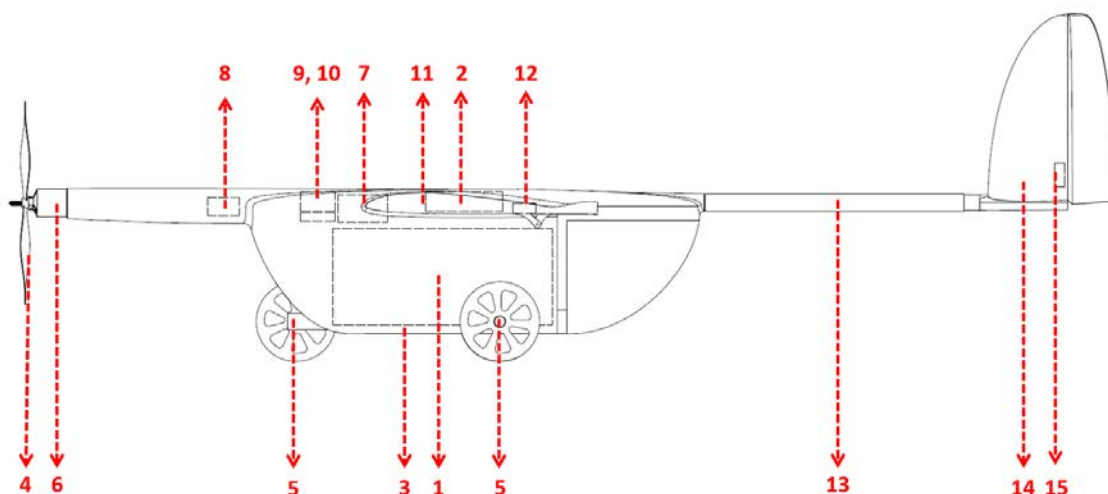


Fig. 5-1 Weight distribution in aircraft

CG position is calculated for maximum payload weight. **CG position stays unchanged for all payload configurations.**



Centre of gravity:

$$x_T = \frac{\sum_1^n m_n \cdot x_{nT}}{\sum_1^n m_n} \quad [mm] \quad (5.1)$$

Due to the origin of the coordinate system:

$$x_T = \frac{3497059}{5000} = 699,5 \text{ mm}$$

Due to the  $C_{MAC}$ :

$$\overline{x_T} = \frac{x_T - x_{aer}}{C_{MAC}} \cdot 100 = \frac{699,5 - 625}{246} \cdot 100 = 30,3\% \quad (5.2)$$

## 6. PAYLOAD PREDICTION

Paying loads are packages of artificial blood of 100, 200 and 300 g. Set requirement is that the loads should primarily consist of the heaviest 300 g packages.

From the flight performance analysis to achieve required climb speed and take-off distance,  $M_{tow}$  was determined to 5 000 g. From the weight analysis aircraft empty weight was calculated about 2 900 g. Then the expected maximum weight of the payload is 2 100 g. Thus, a combination of seven packages of 300 g was chosen as maximum payload. But other configurations are possible- see Tab.6.1. CG position stays unchanged for all payload configurations.

It was decided to shelve the payload in the way shown on the Fig.6.1. This decision was made because of liquidity of the blood packages. Blood bag storage in this way prevents from overflow and minimize the liquid movement in the airplane. This position is considered to be the safest option for flight.

Tab. 6.1 Payload shelving options

Number of packages	Weight [g]	Shelving option
1	300	
2	600	
3	900	
4	1200	
5	1500	
6	1800	
7	2100	

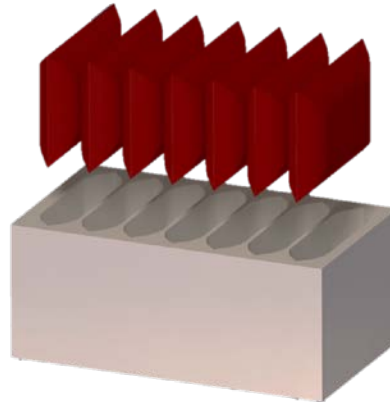


Fig. 6-1 Payload overview

## 7. FLIGHT PERFORMANCE

All calculated flight performance are made with aircraft at maximum take-off weight.

### 7.1 Thrust measurement

The measurement was performed with a JETI MEZON 55 PRO controller, AXI 2826/10 motor, and a 12V 400 Ah lead-acid battery. The measured propeller is Aeronaut CAM Carbon 10x6. The measurement result is shown in Figure 5-1.

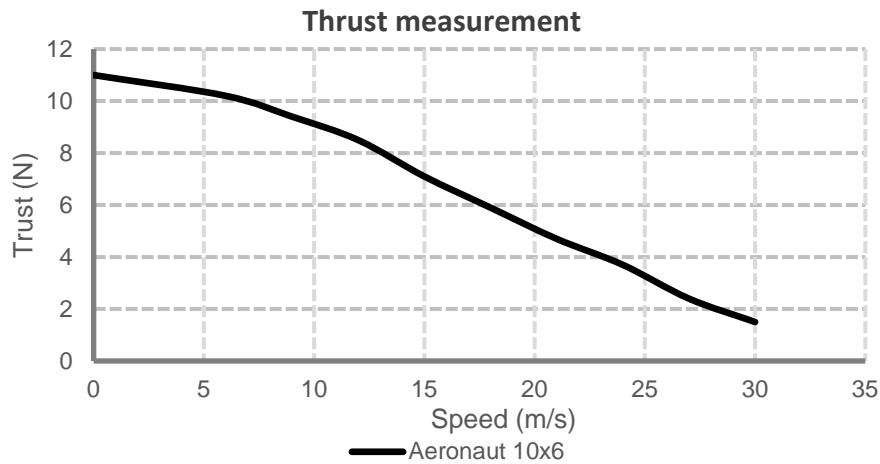


Fig. 7-1 Thrust measurement

### 7.2 Horizontal flight

In horizontal flight, the following forces act on the aircraft:

$$x: F - D = 0 \quad [N] \quad (7.1)$$

$$z: L - G = 0 \quad [N] \quad (7.2)$$

To determine the performance characteristics of the aircraft, an analytical polar was created by calculation, where the drag coefficient at zero lift coefficient was determined so that these values correspond to the values from the XFLR5 program.

$$c_D = c_{D_m} + \frac{(c_L - c_{Lm})^2}{\pi A e} \quad [-] \quad (7.3)$$



Where

$$c_{Lm} = 0,168529$$

$$c_{Dm} = 0,009315$$

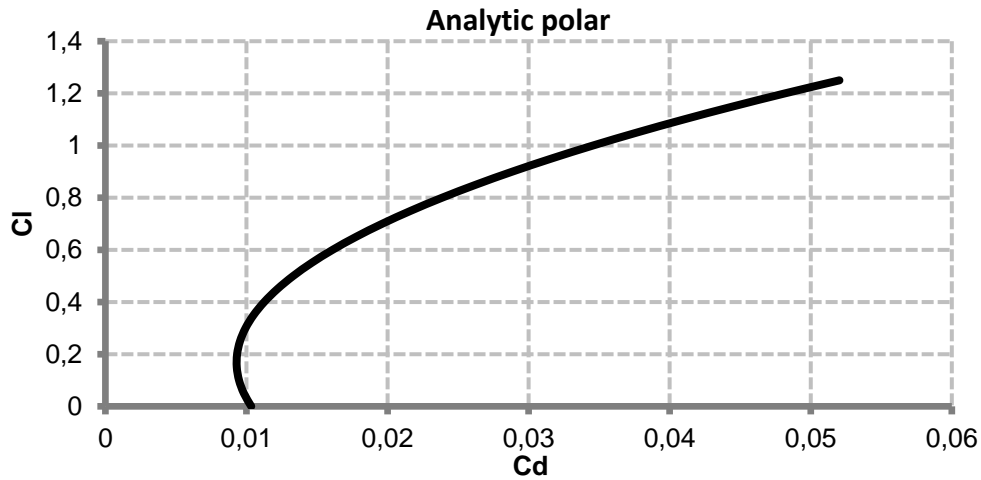


Fig. 7-2 Flight polar

Based on the information obtained, graphs of usable and required performance are plotted. See Fig.7-3.

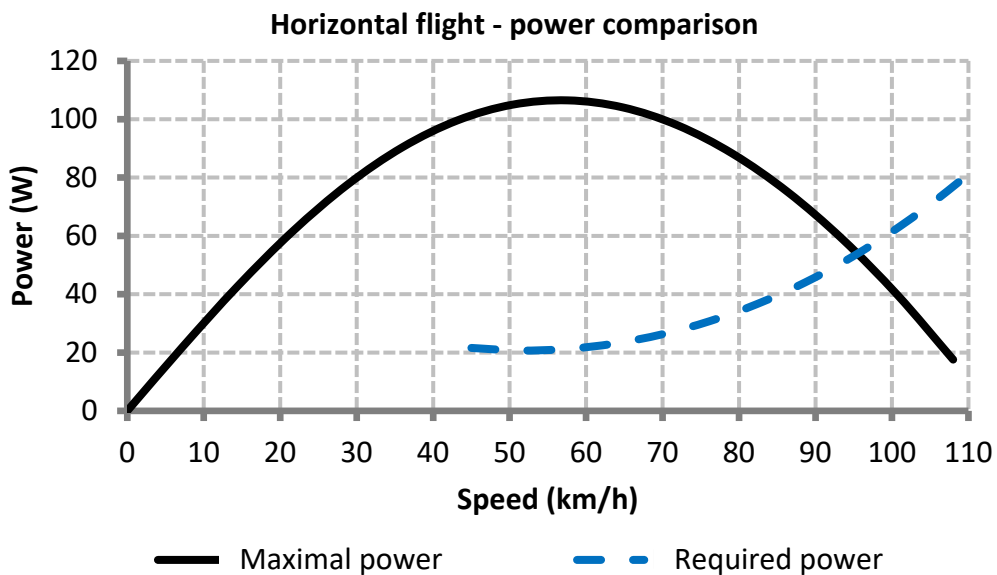


Fig. 7-3 Horizontal flight - power comparison

### 7.3 Climb

In steady climb following forces act on the aircraft:

$$x: F - D - G \sin \gamma = 0 \quad [N] \quad (7.4)$$

$$z: G \cos \gamma - L = 0 \quad [N] \quad (7.5)$$

From the knowledge of excess power, the dependence of climb speed on flight speed can be determined. The following relationship was used:

$$w = \frac{\Delta P}{G} \quad [ms^{-1}] \quad (7.6)$$

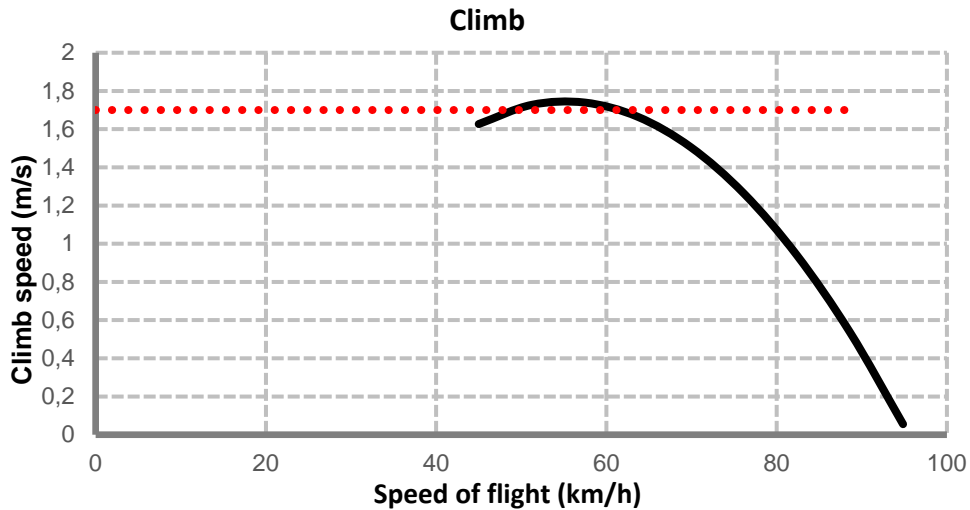


Fig. 7-4 Climb

The required climbing speed was determined from the competition rules. In order to achieve the largest possible number of points, it is necessary to climb 100 m in 60 s. It follows that the required climb speed is equal to:

$$v_{climb} = \frac{s}{t} = \frac{100}{60} = 1,667 \quad [ms^{-1}] \quad (7.7)$$

The longitudinal slope of the track is determined by:

$$\gamma = \sin^{-1} \frac{F - D}{G} \quad [^\circ] \quad (7.8)$$

or

$$\gamma = \sin^{-1} \frac{W}{v} \quad [^\circ] \quad (7.9)$$

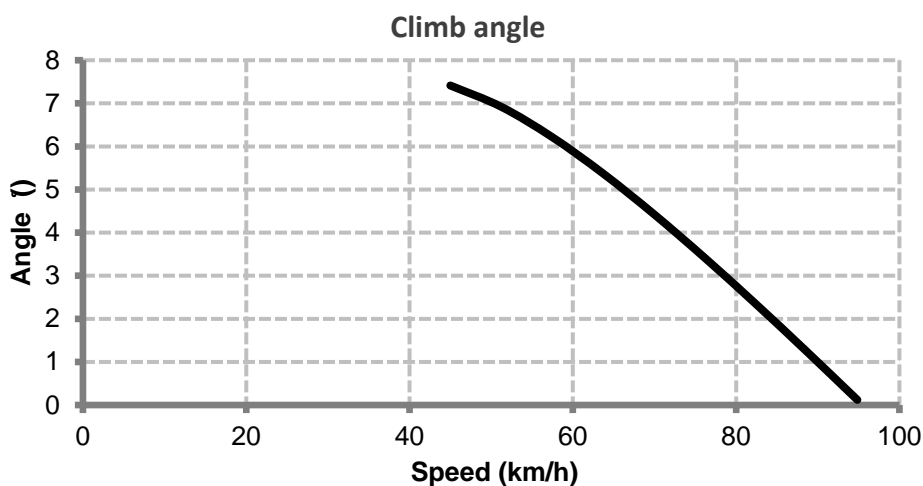


Fig. 7-5 Climb angle

#### 7.4 Take off

The drag coefficient is subtracted from the XFLR5 program. According to the competition rules, the takeoff on the grass is performed. To achieve bonus points take-off on 40 meter long runway is chosen.

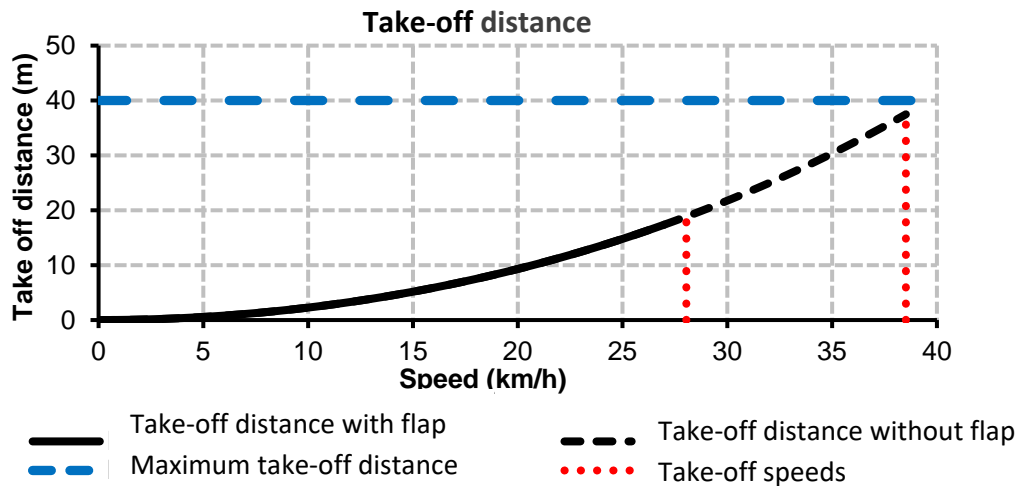


Fig. 7-6 Take-off

## 8. STABILITY

Aircraft stability is calculated according [6]. Only resulting equations and results are displayed in this chapter.

Resulting position of the aerodynamic center:

$$\bar{x}_A = \bar{x}_{AKT} + \Delta\bar{x}_{HT} \quad [-] \quad (8.1)$$

$$\bar{x}_A = 0,2471 + 0,1504 = 0,3975$$

Static reserve:

$$\sigma_A = \bar{x}_A - \bar{x}_T = 0,3975 - 0,302 = 0,0955 \quad [-] \quad (8.2)$$

For moment curve applies:

$$c_{mK} = c_{m0K} + c_{m\alpha K} \cdot (\alpha_{KT} - (\alpha_{0KT} - \varphi_K)) \quad [-] \quad (8.3)$$

where  $c_{m\alpha K}$  :

$$c_{m\alpha K} = a_K \cdot (\bar{x}_T - \bar{x}_{AK}) \quad [1/rad] \quad (8.4)$$

Resulting moment curve is displayed in Fig. 4-1. Moment curve was calculated according [6] and also calculated in XFLR5. For all configurations the airplane is stable. **CG position stays unchanged for all payload configurations.**

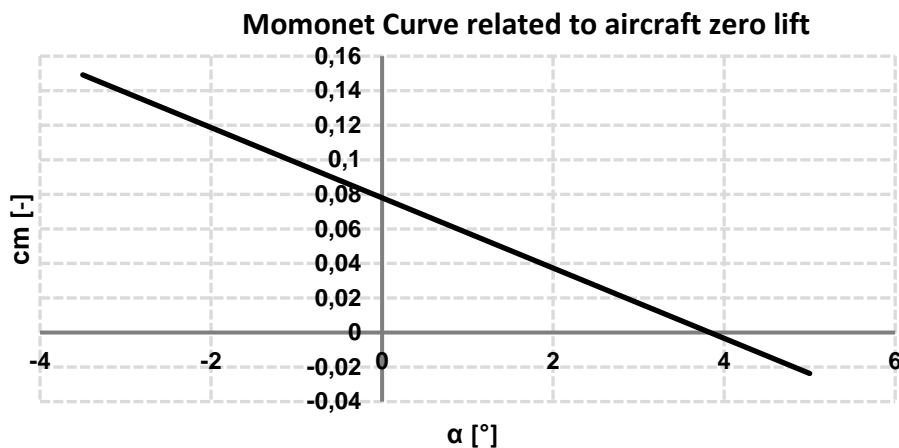


Fig. 8-1 Moment Curve



## 9. STRUCTURAL DESIGN

This chapter discusses the design of the internal structure of the airplane. The competition does not restrict the use of any materials. The design of the structure also takes into account that the model must be disassembled so that all its parts fit into the transportation box.

In aircraft construction is used multiple kinds of materials, mostly carbon and glass fabric, plywood and balsa wood, PLA plastic, aluminum alloys.

With help of laser cutting technology, it is able to achieve precise shapes and profiles, such as ribs, in very short time from any kind of wood.

For the construction of aircraft safety factor value 1,5 is used. This value is typically use for aircraft design.

Tab. 9.1 Materials

Material	Density [kg/m <sup>3</sup> ]	Application example
<b>Plywood</b>	512,5	flanges, ribs, stringers
<b>Balsa wood</b>	130	wing spar, tail unit
<b>Cover plastic foil</b>	0.000596 [kg/m <sup>2</sup> ]	wing, tail unit - skin
<b>5 minutes EPOXY</b>	147	fastener
<b>Super glue</b>	1060	lightly loaded parts
<b>PLA plastic</b>	1250	3D printed parts
<b>Carbon fabric</b>	90 [g/m <sup>2</sup> ]	D-box, flap, fuselage
<b>Glass fabric</b>	100 [g/m <sup>2</sup> ]	fuselage

### 9.1 Flight envelope

The flight envelope is calculated on the basis of calculations from the CS-VLA regulation [8], this regulation deals with very light airplanes. The flight envelope is used to determine the speeds and loads that may occur during the flight.

Tab. 9.2 Design airspeeds

Design airspeeds	Speed [km/h]	Load factor n	Gust n
<b>Cruise speed</b>	85,56	—	—
<b>Stalling speed</b>	39,21	1	—
<b>Manoeuvring speed</b>	76,42	3,8	7,0
<b>Stalling speed – negative load factor</b>	54,45	1	—
<b>Manoeuvring speed– negative load factor</b>	66,68	-1,5	-5
<b>Dive speed</b>	106,95	3,8	5,5
		-1,5	-3,5
<b>Max. speed with flaps fully deflected</b>	54,88	2	—
<b>Stalling speed with flaps fully deflected</b>	28,04	1	—
<b>Manoeuvring speed with flaps fully deflected</b>	39,65	2	—

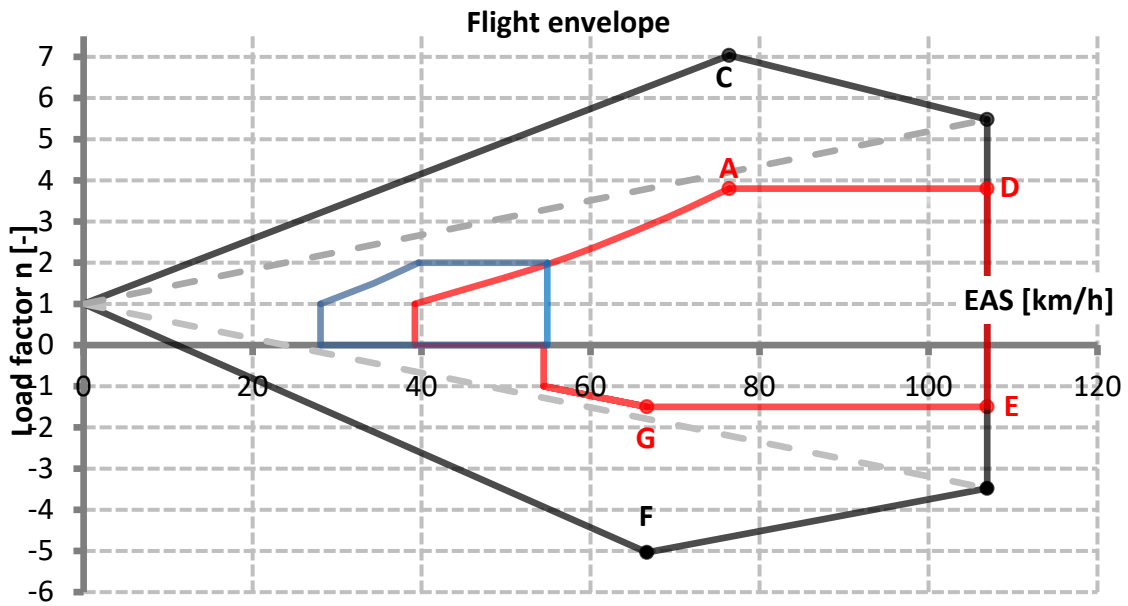
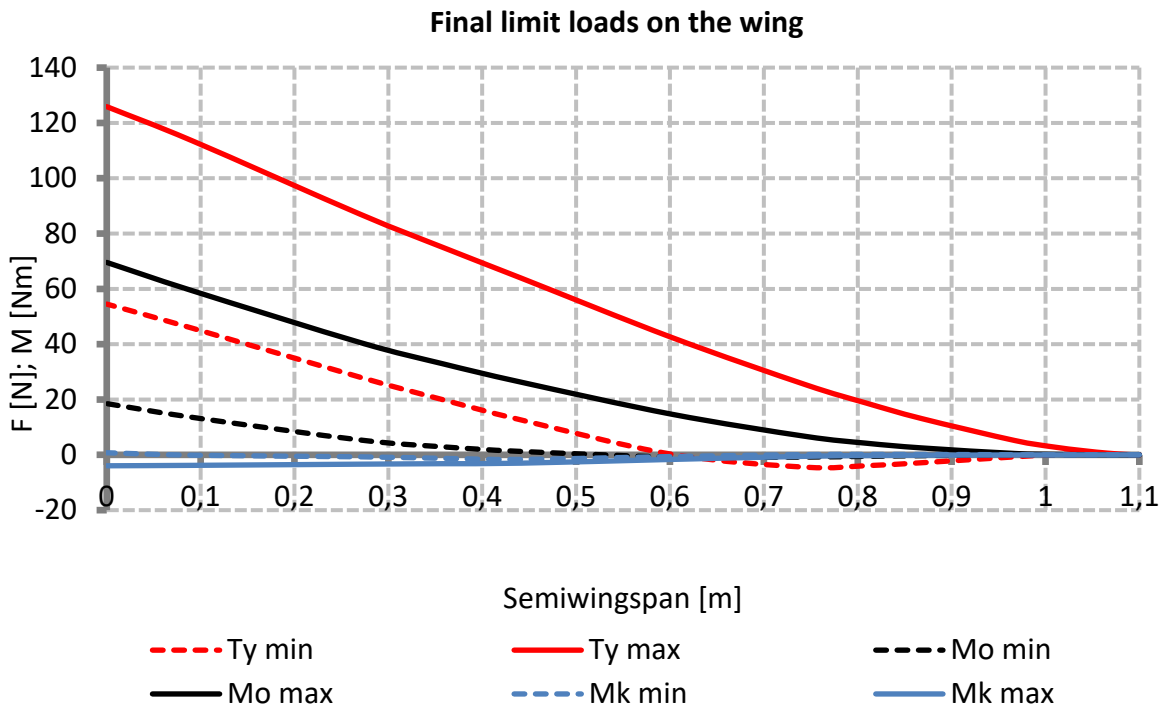


Fig. 9-1 Flight envelope

### 9.2 Wing design

When calculating the load on the wing, the gust load is not taken into account, as it is not expected to fly in such conditions. It would also result in an undesirable increase in the weight of the overall wing structure, which would mean a decrease in the weight of the carried weight. The wing load calculation was calculated using numerical integration. Program Excel was used to calculate and plot the graphs. Final extreme load on the wing is displayed on the Fig. 9-2.



Ty – shear force; Mo- bending moment; Mk – torsion moment

Fig. 9-2 Wing limit loads



Wing structure design is displayed on the Fig. 9-3.

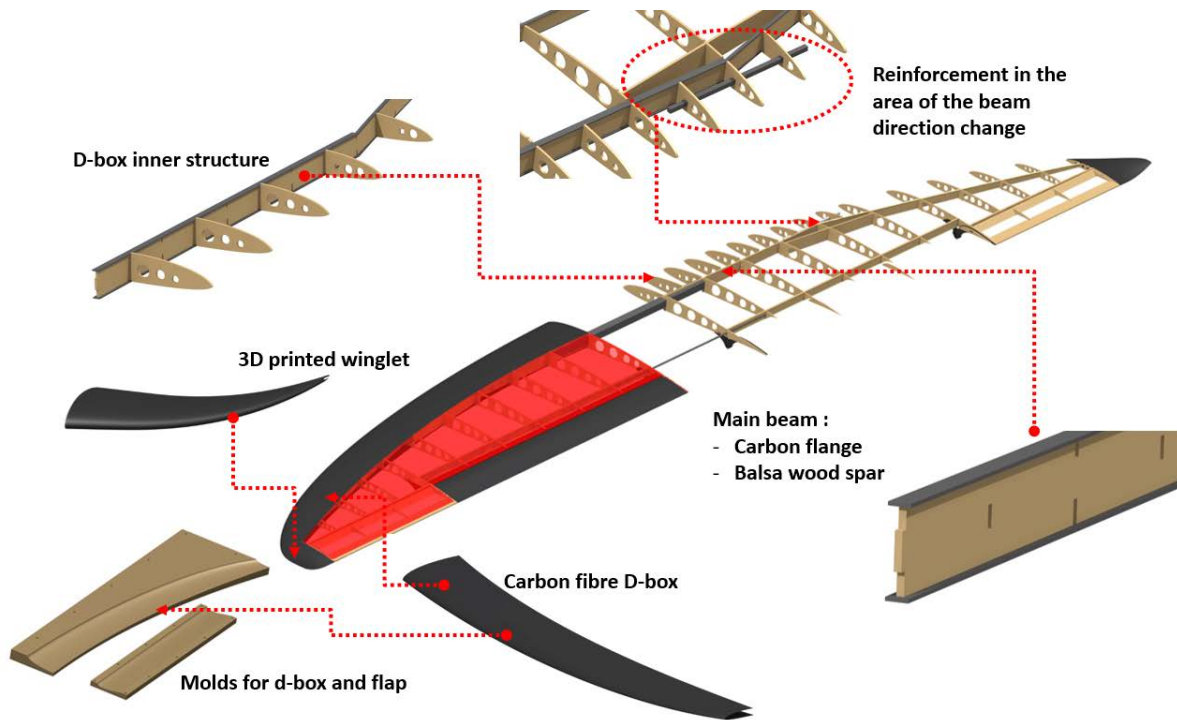


Fig. 9-3 Wing structure

- **D-box**

To keep the structure firm, strong and light enough, proper material selection is a vital aspect. Due to its complexity, the carbon fibre composite and glass fibre composite were chosen as the best material for the D-box construction. It has high strength, low weight, however the most important characteristic is good formability during manufacturing.

- **Main spar design**

The wing is replaced by a model of a single-girder single-cavity construction with two flanges.

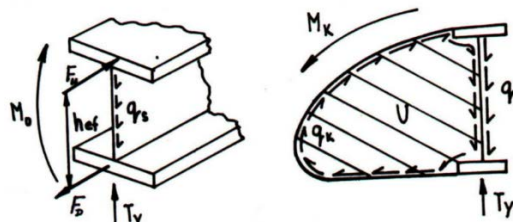


Fig. 9-4 Spar

The stress on the individual parts of the spar was calculated. The selected parameters are listed in the Tab.9.3.

Tab. 9.3 Wing spar parameters

Parameter	Label	Value	Unit
Construction height of the root chord	$h_{s,cr}$	26,406	mm
Effective height of the root chord	$h_{ef,cr}$	25,406	mm
Flange height	-	1	mm
Flange width	-	6	mm
Web width	$t_{web}$	2	mm
Safety factor	$k$	6,25	-

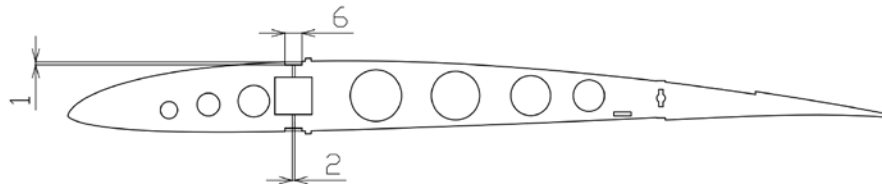


Fig. 9-5 Root rib

- **Ribs**

These elements form the basic transverse support system. The basic tasks of these elements include securing the required shape, capturing some partial loads, separating the interior spaces, reinforcing the edges of the holes. The number of ribs 11 was chosen for the half-span. In the D-box of the wing in the initial part, 5 pieces of items are added to strengthen the D-box cover. The ribs will be cut with plywood or balsa wood.

- **Wing connection**

The wing is connected by a carbon rod, which can be seen in Figure 8-7. It passes through the model's fuselage where it is secured.



Fig. 9-6 Wing connection

safety factor of the connector:  $k = 1,023$

### 9.3 Tail design

Fig. 9-7 below shows final limit load on the tail. The gust load is not taken into account. It would also result in an undesirable increase in the weight of the overall tail structure. The tail load calculation was calculated using numerical integration.

- Tail inner structure is made mainly of plywood and balsa wood.
- Carbon is used for the flanges, connection rod and tail connector to the fuselage.

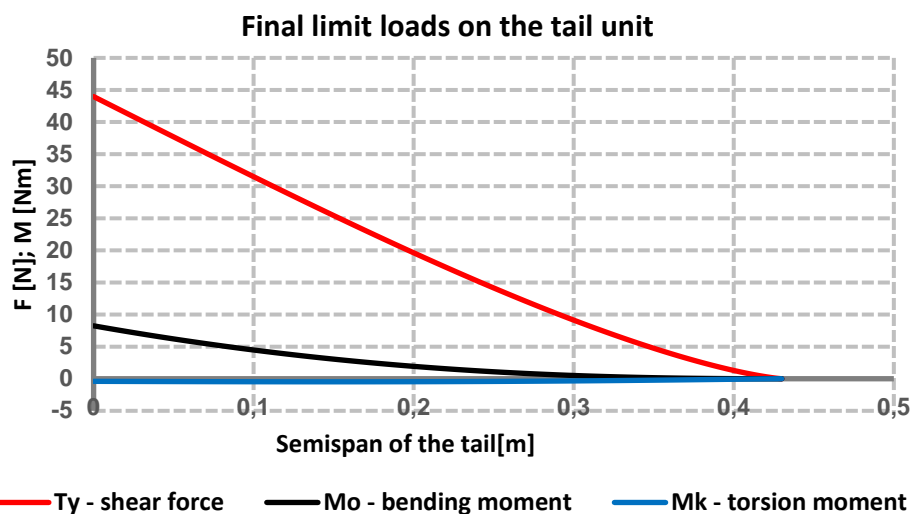


Fig. 9-7 Final limit loads - tail



Tab. 9.4 Tail spar parameters

Parameter	Label	Value	Unit
Construction height of the root profile	$h_{s\ cr\ tail}$	12,24	mm
Effective height of the root profile	$h_{ef\ cr\ tail}$	9,24	mm
Flange height	-	1	mm
Flange width	-	3	mm
Web width	$t_{web\ tail}$	3	mm
Safety factor	$k$	6,3	-

- Ribs and main structure are made with laser cutting method.
- Tail tip is made with 3D printed parts.
- Main connection to the fuselage is made from carbon fibres in the 3D printed molds and core of this connector is also 3D printed.

Fig.9-8 below shows inner structure of the tail unit.

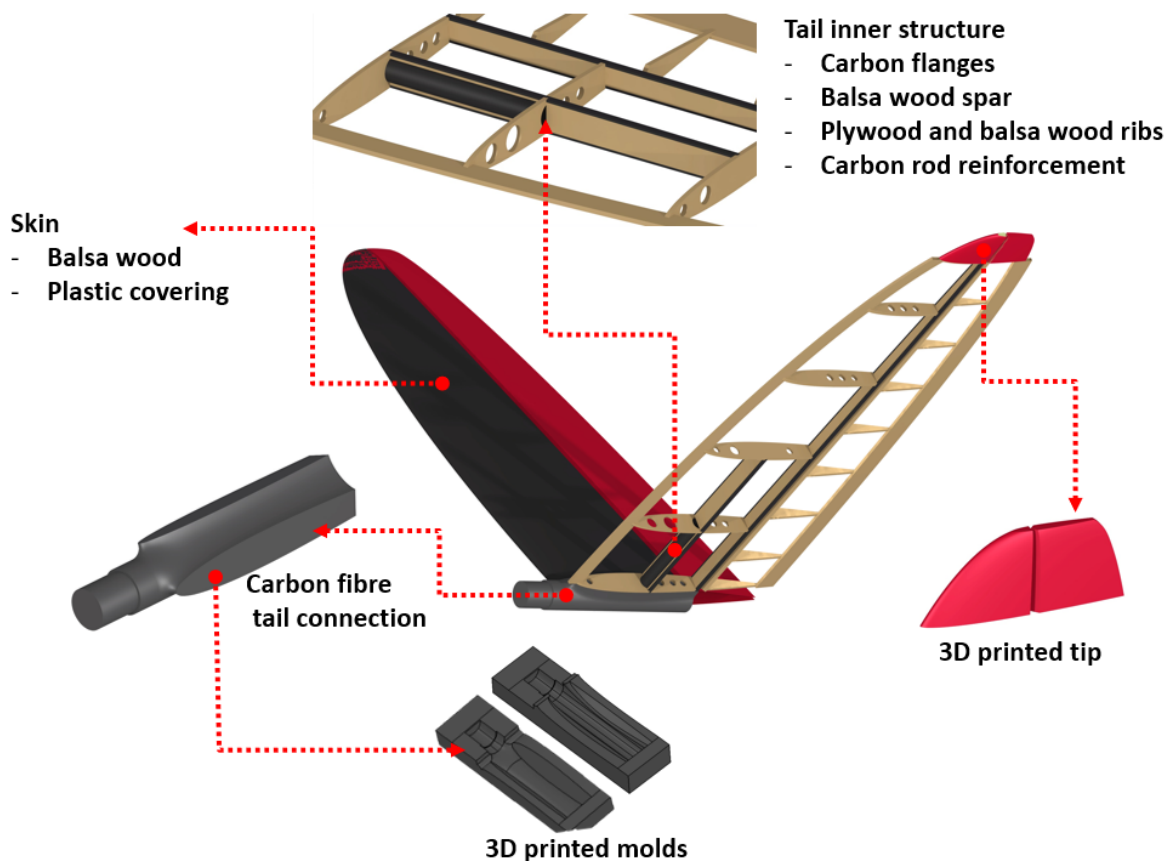


Fig. 9-8 Tail inner structure



## 9.4 Fuselage and landing gear design

Fuselage structure is shown on the Fig.9-9. The gondola consists of two separate parts. The major supporting part has a purpose of attaching the payload and attaching the main landing gear. The back part is a removable aerodynamic cover. The cover is attached to the supporting part with a small neodymium magnets.

- The aerodynamic shape of the gondola is made from glass fibre and is reinforced with plywood stringers – they provide enough support for whole cargo and electronics.
- Payload- the blood bags are placed into the plywood box to secure them on place without possible movement.
- For the rear part of the fuselage the carbon rod is used. The rod is connected to the main fuselage part with two screws. See Fig. 9-9 below.
- In the main fuselage part, the automated measuring box with requested dimensions is used. The telemetry (automated measuring box) is placed on the top of the aircraft leading to the sky.
- Payload is inserted and removed through the removable cover part of the fuselage.
- The payload secure system used at the ACC 2019 by our team is considered the most effective and fastest solution. This system is used again and is shown on the Fig. 9-10.

Landing gear is made from aluminium tubes. It is mount with the screws to the fuselage inner structure. The maximum load on the fuselage was tested and the construction provided enough stiffness.

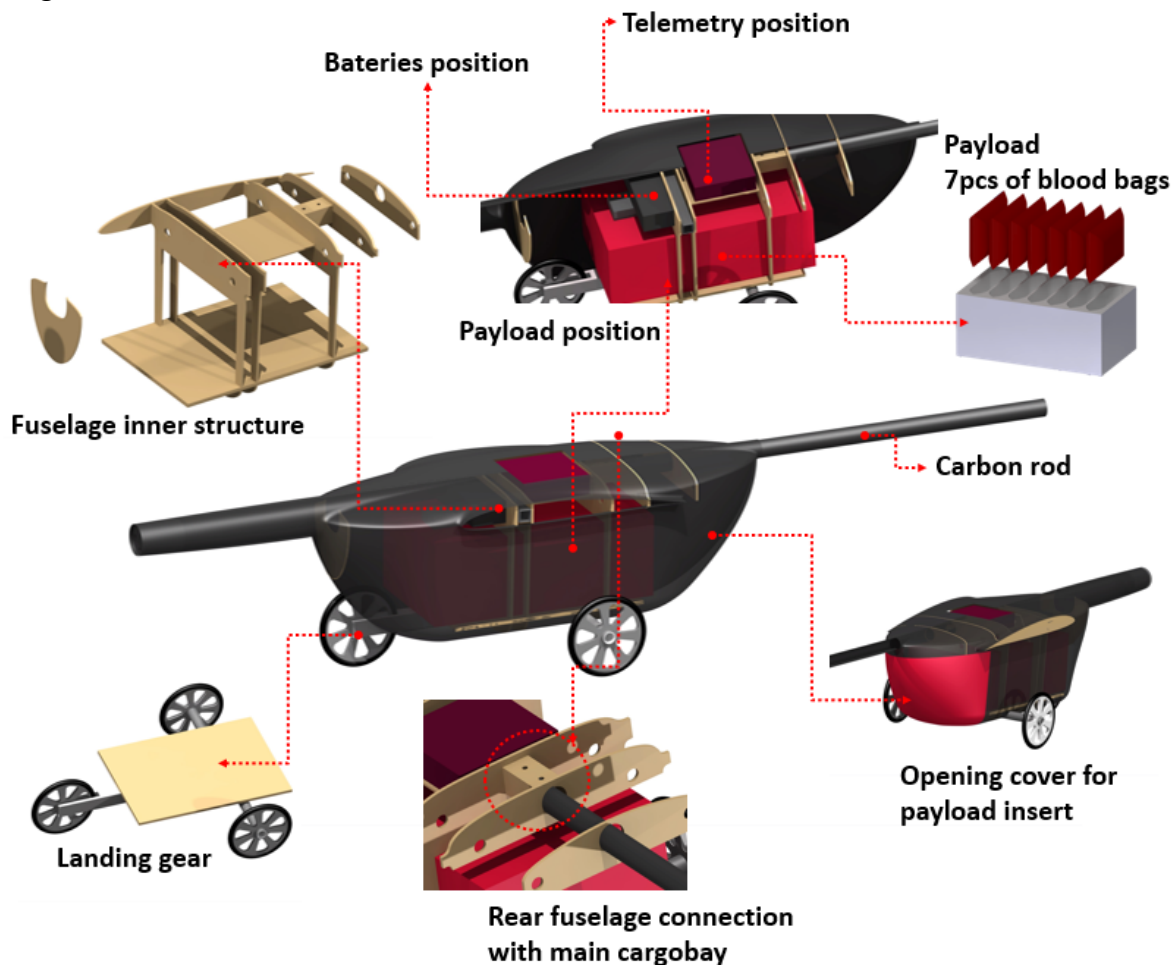


Fig. 9-9 Fuselage structure

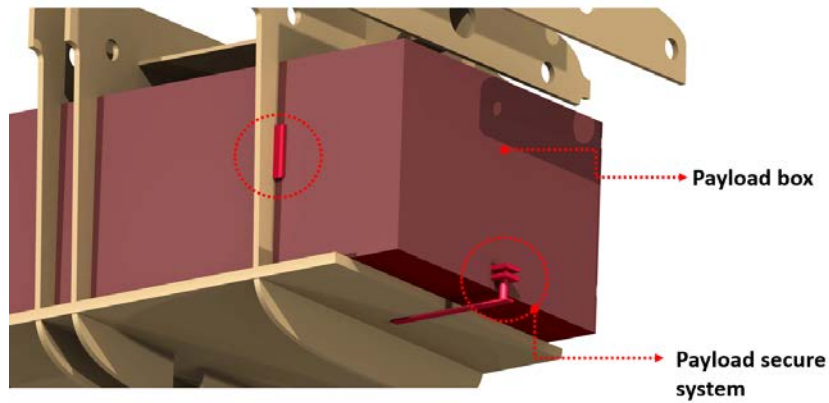


Fig. 9-10 Payload secure system

## 10. FINAL DESIGN SUMMARY

Tab. 10.1 Aircraft parameters

Part	Parameter	Value	Unit
<b>Wing</b>	Wing area	0,5	m <sup>2</sup>
	Wingspan	2200	mm
	Root chord length	290	mm
	Air foil	S9000_S7075	-
	Mean aerodynamic chord length	246	mm
	Aspect ration	9,66	-
<b>Empennage</b>	Empennage area	0,11	m <sup>2</sup>
	Root chord length	158	mm
	Span	720	mm
	Air foil	NACA 0010	-
	Horizontal tail volume	0,465	-
	Vertical tail volume	0,022	-
<b>Aircraft</b>	Total length	1395	mm
	Total height	436	mm
	Maximal take-off weight	5000	g
	Empty weight	2900	g



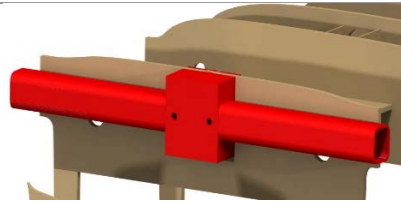
Fig. 10-1 Aircraft visualisation



## 11. DIFFICULTIES DURING THE PROJECT, INNOVATIONS

ACC 2022 aircraft is Chicken Wings seventh model built over the years. The team learned from each project and this project is no exception. The primary goal in the building process was to build the light weighted construction as possible. Tab.11.1 below shows difficulties and new methods used.

Tab. 11.1 Difficulties and innovations

No.	Description	Picture	Result
<b>Innovations</b>			
1	Empennage and rear fuselage connection. For connection 3D printed molds were made. To find the best option – lightweight but durable three prototypes were made.		Success 😊 ✓
2	Wing connection case. As material for the case the glass fibre was used. Process – the carbon rod was covered with glass fibre and then the rod was removed. The case was used on first wing prototype – significant clearance. Replaced with 3D print and balsa.		Fail 😞 ✗
<b>Difficulties</b>			
3	First wing prototype destroyed during static test – used glue was absorbed to the balsa wood, not enough adhesion with d-box. Solution – different type of glue was used.		Success 😊 ✓
4	During the building process the angle on semispan differ. The case for the connection in the fuselage middle part maintains the right angle. Result – the wing connector – carbon rod split.		Success 😊 ✓

## 12. OUTLOOK

Building process starting at the of September 2021. Currently after six months of milling, grinding, laser cutting, laminating, and the whole building process the aircraft is at the final stage. The team is working on the last details like wheels optimisation etc. The flights should start at the begging of month May 2022 so that the pilot and the team are given enough time to practice with the airplane and spot possible flaws.

In the attachment of this document the photos and related pictures to aircraft and building process are displayed.



## LITERATURE AND REFERENCE LIST

- [1] Air Cargo Challenge 2021 Regulations. *Aka Model Munchen* [online]. 2020 [cit. 2022-4-14]. Available from: <https://akamodell-muenchen.de/acc-2022/regulations/>
- [2] OLŠANSKÝ, Oldřich a Jiří MATĚJČEK. Konstrukce a výpočet ultralehkých letounů. Praha: Letecká amatérská asociace ČR, 1999
- [3] GUDMUNDSSON, Snorri. General aviation aircraft design: applied methods and procedures. Oxford: Elsevier, 2014. ISBN 978-0-12-397308-5.
- [4] DANĚK, Vladimír. Mechanika letu I. Brno: Akademické nakladatelství CERM, 2009. ISBN ISBN978-80-7204-659-1.
- [5] DUŠAN SLAVĚTÍNSKÝ, Dušan. O letadlech [online]. [cit. 2022-04-14]. Available from : <http://www.slavetind.cz/Default.aspx>
- [6] DANĚK, Vladimír.: Mechanika Letu II: Letové vlastnosti. Brno: Akademické Nakladatelství CERM,s.r.o., 2011. ISBN 978-80-7204-761-1.
- [7] ROSKAM, Jan. Airplane design: PartVI:Preliminary calculation of aerodynamics thrust and power characteristic, The University of Kansas, 1987.
- [8] CS-VLA: CERTIFIKAČNÍ SPECIFIKACE PRO VELMI LEHKÉ LETOUNY. *Úřad pro civilní letectví* [online]. 2009 [cit. 2022-4-14]. Available from: [https://www.caa.cz/wp-content/uploads/2019/07/CS-VLA\\_konsolidovane\\_amdt\\_1\\_opr1CR\\_CZ.pdf?cb=77510d8c9f6734ddbba1d389a759472](https://www.caa.cz/wp-content/uploads/2019/07/CS-VLA_konsolidovane_amdt_1_opr1CR_CZ.pdf?cb=77510d8c9f6734ddbba1d389a759472)
- [9] PETRÁSEK, Miloslav. Konstrukce letadel II. Brno: Univerzita obrany, 2011. ISBN 978-80-7231-212-2.
- [10] *Model Motors: AXI* [online]. [cit. 2022-04-30]. Available from: <https://www.modelmotors.cz/product/detail/394/>



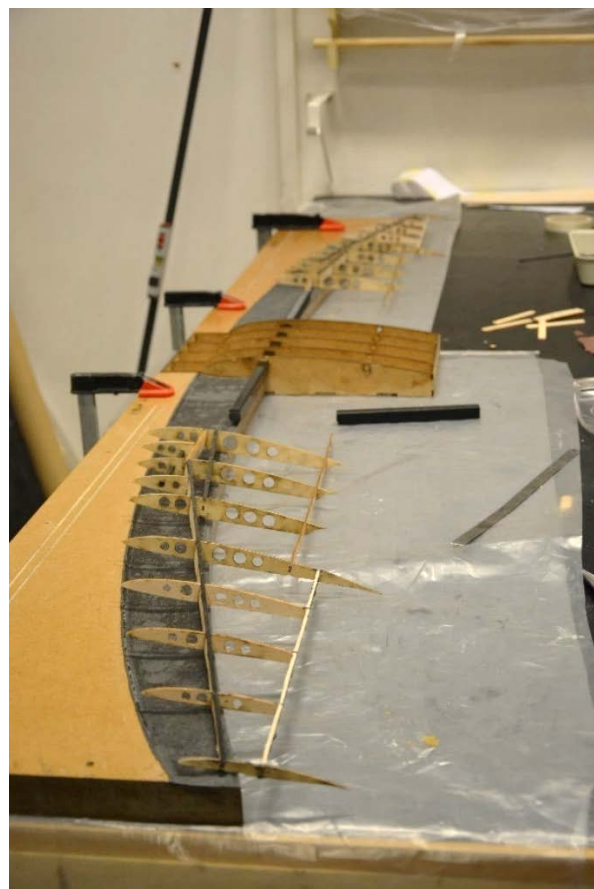
## Attachment



Attachment A : Position in transportation box



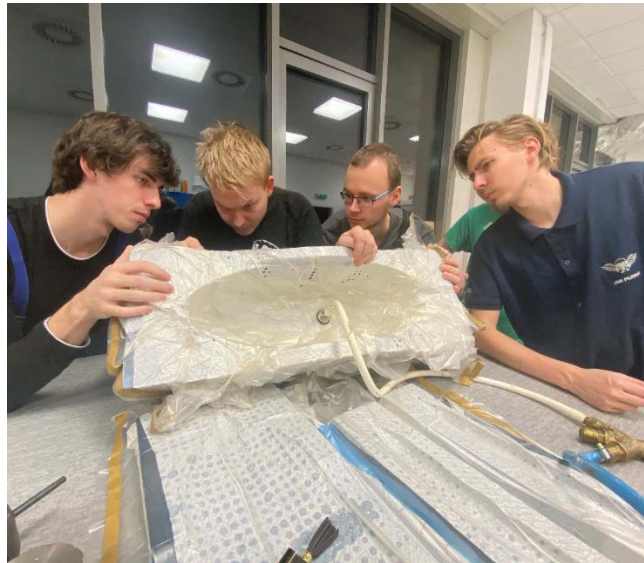
Attachment B Molds preparation



Attachment C Wing structure



Attachment D Gondola lamination



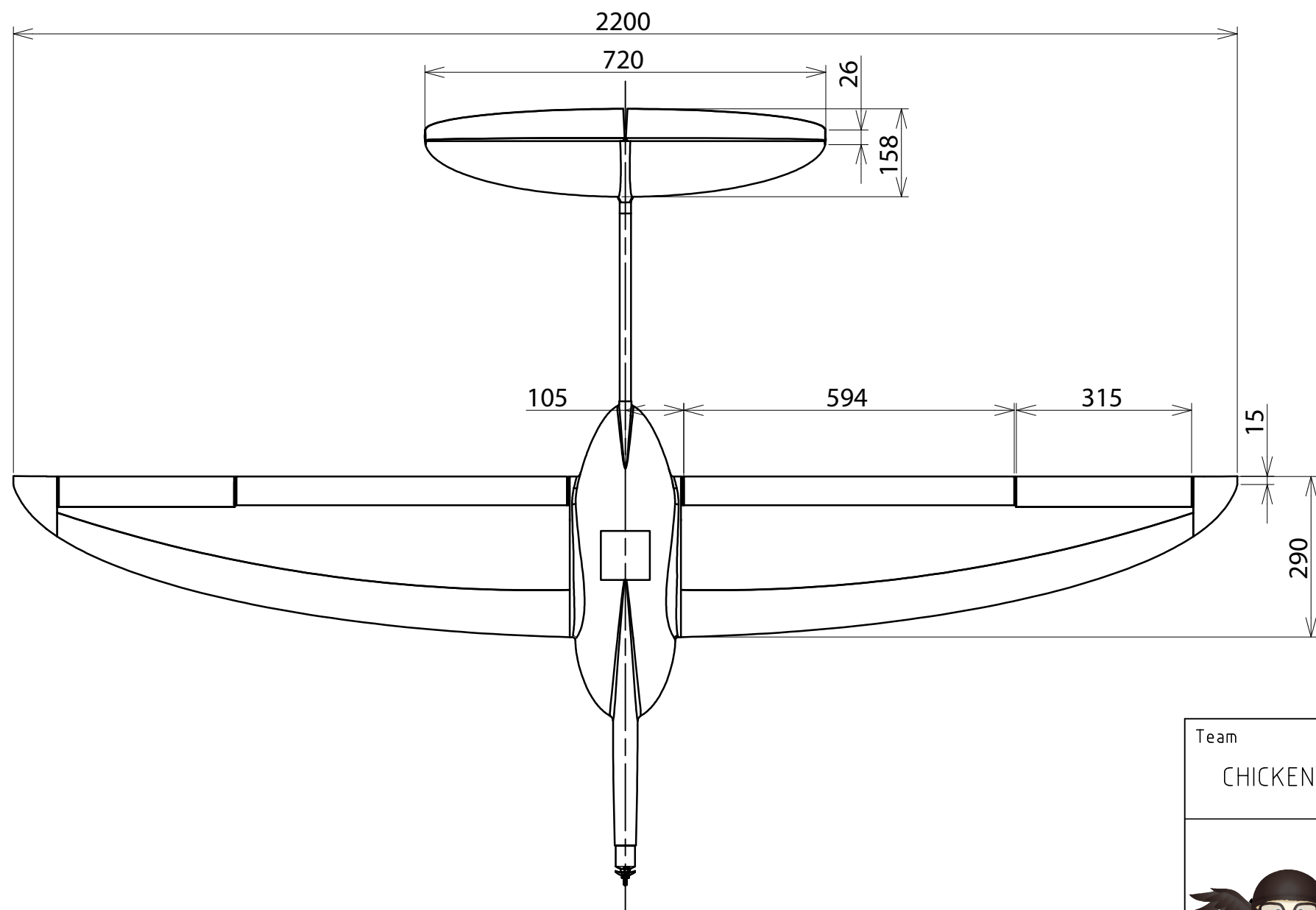
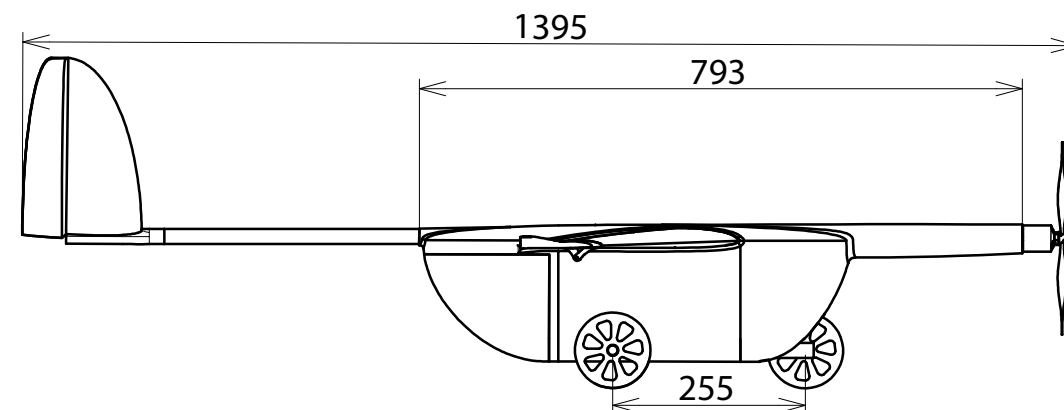
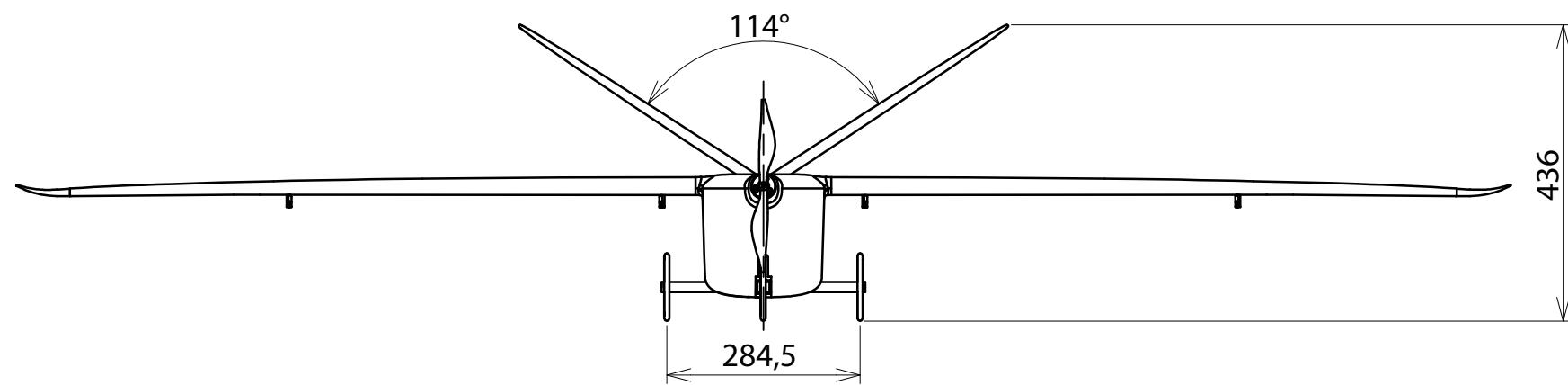
Attachment E Gondola pressed



Attachment F Wiring installation



Attachment G Aircraft preparation



OTHER DIMENSIONAL INFORMATION

Empty weight	2900 g
Maximum take-off weight	5000 g
Centre of Gravity position (for all configuration % MAC)	30,3 %

Wing Parameters

Wing Area	0,5 m <sup>2</sup>
Root Airfoil	S9000
Second Airfoil	S7075
Second Airfoil wing span position	700 mm
Mean aerodynamic chord length	246 mm
Mean geometric chord length	227,3 mm

Empennage parameters

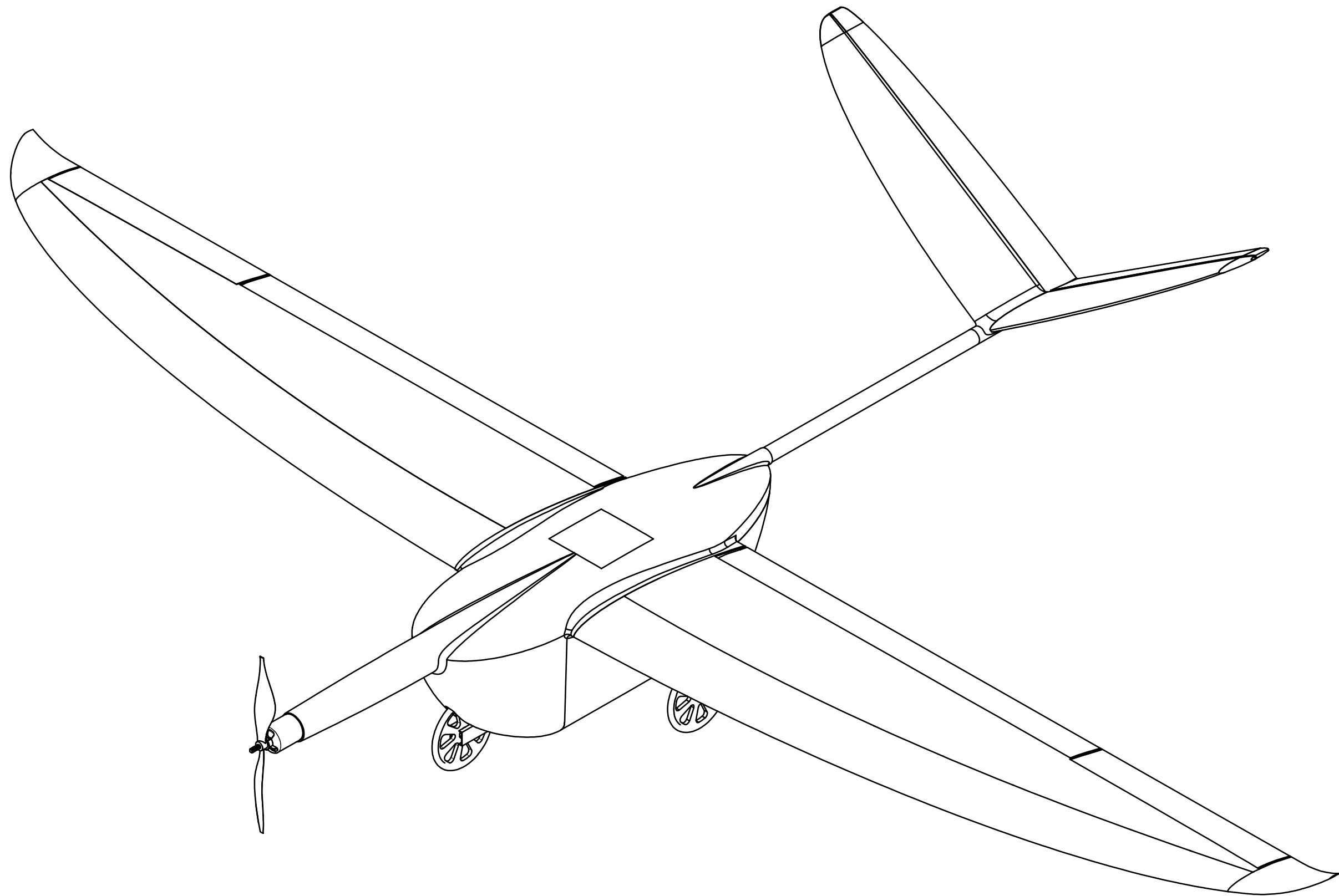
Empennage Airfoil	NACA 0010
Empennage Area	0,11 m <sup>2</sup>
Horizontal stabilizer Area	0,077 m <sup>2</sup>
Horizontal stabilizer Volume	0,4650
Vertical stabilizer Area	0,033 m <sup>2</sup>
Vertical stabilizer Volume	0,0223

Fuselage parameters

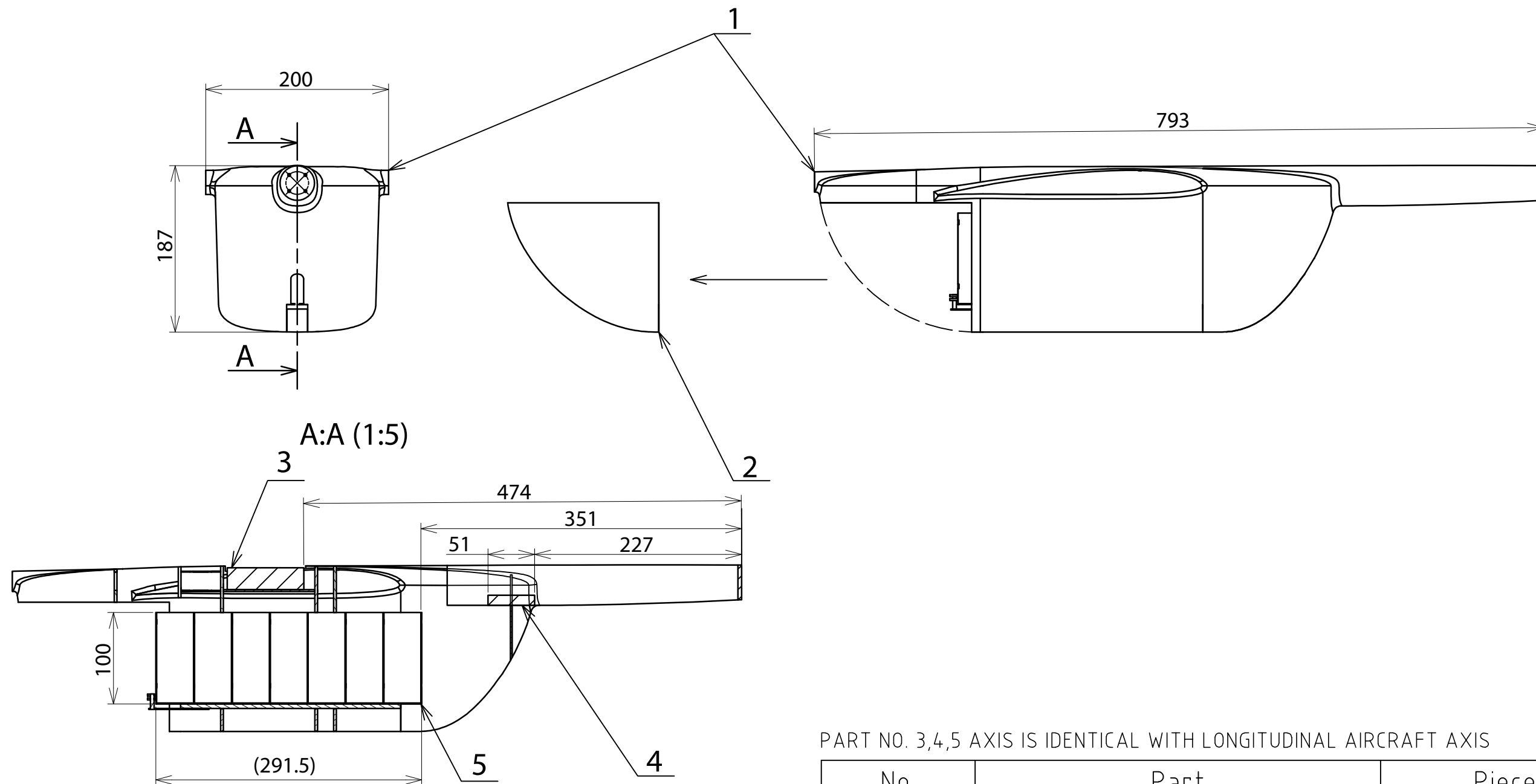
Fuselage Airfoil	E863
------------------	------

Team	University	Team number	Scale
CHICKEN WINGS BUT	Brno University of Technology	05	1:10

	Drawn	Radim Machac	Title	3-VIEW DRAWING
	Released	Tatiana Kminiakova		
	Date	29.04.2022	Drawing No.	CHW0001N
	Drawing Size	A3		

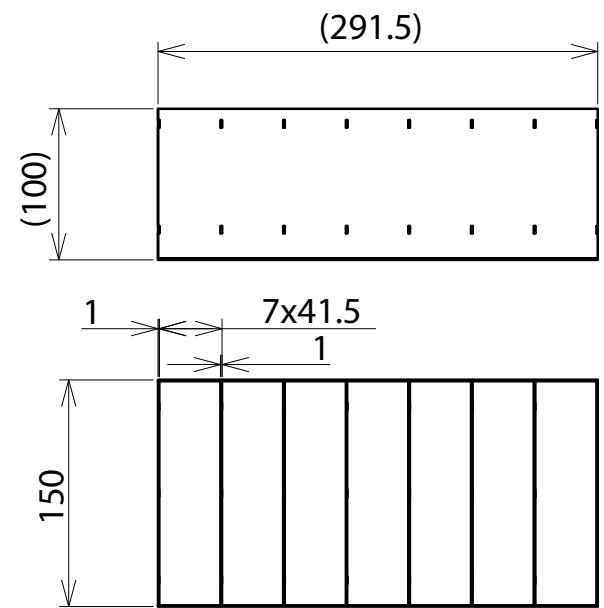


Team	University	Team number	Scale
CHICKEN WINGS BUT	Brno University of Technology	05	1:5
	Drawn	Title	
	Released	ISOMETRIC DRAWING	
	Date	Drawing No.	
	Drawing Size	CHW0002N	
	A3	Sheet 2 / 4	



A:A (1:5)

CARGOBAY (1:5)

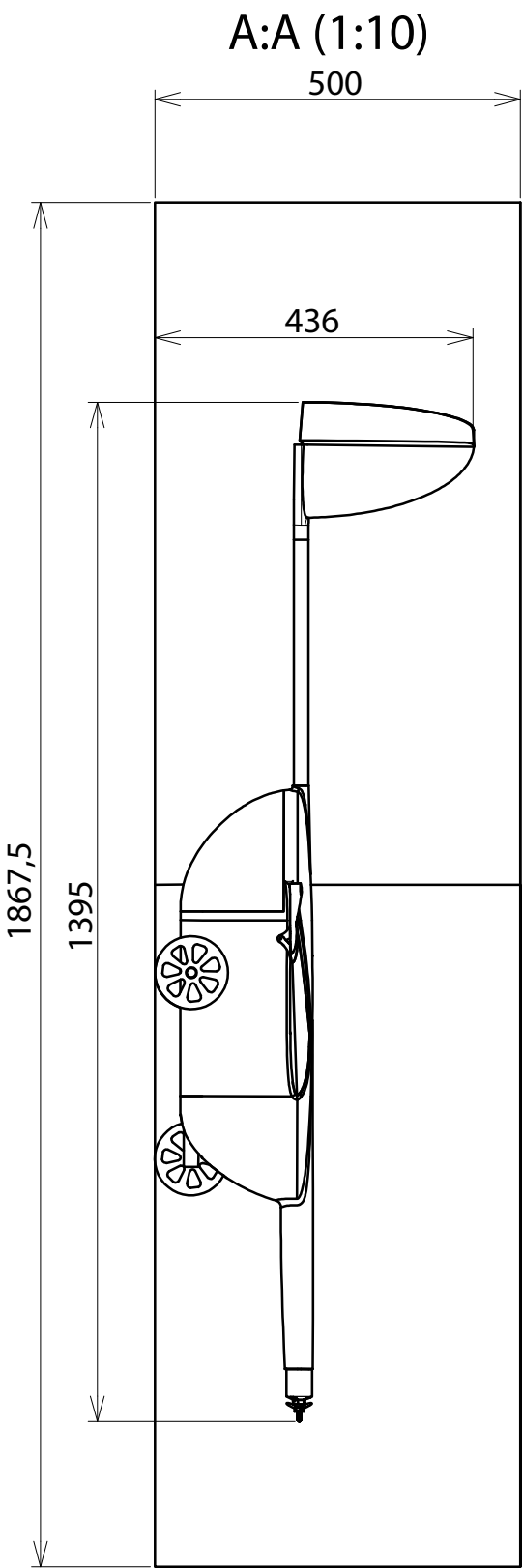
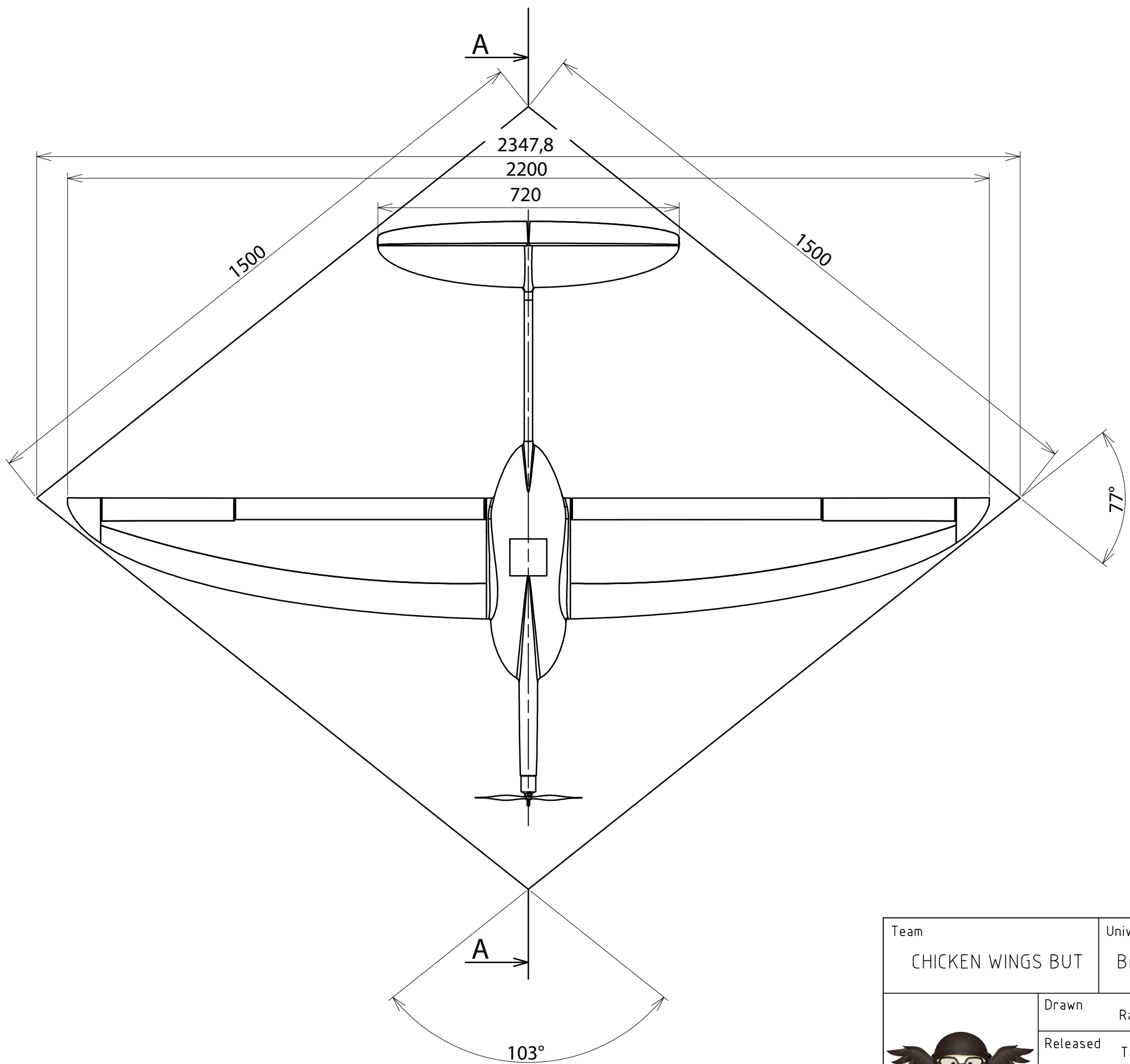


PART NO. 3,4,5 AXIS IS IDENTICAL WITH LONGITUDINAL AIRCRAFT AXIS

No.	Part	Pieces
1	Fuselage	1
2	Fuselage cover	1
3	Measuring equipment	1
4	RC Receiver	1
5	Cargobay	1

Team CHICKEN WINGS BUT	University Brno University of Technology	Team number 05	Scale 1:5
---------------------------	---	-------------------	--------------

	Drawn Radim Machac	Title CARGOBAY, RC RECEIVER MEASURING EQUIPMENT
	Released Tatiana Kminiakova	
	Date 29.04.2022	Drawing No. CHW0003N
	Drawing Size A3	



Team	University	Team number	Scale
CHICKEN WINGS BUT	Brno University of Technology	05	1:10
	Drawn	Title	
	Released	READY TO FLIGHT BOX	
	Date	Drawing No.	
	Drawing Size	CHW0004N	
			Sheet 4/4